Molecular Pharmacology Fast Forward. Published on June 20, 2013 as DOI: 10.1124/mol.113.087346
Molecular Pharmacology Fast Forward. Published on June 20, 2013 as doi:10.1124/mol.113.087346
This article has not been copyedited and formatted. The final version may differ from this version.

α4α6β2* nAChR activation on VTA DA neurons is sufficient to stimulate a depolarizing conductance and enhance surface AMPA receptor function

Staci E. Engle, Pei-Yu Shih, J. Michael McIntosh, and Ryan M. Drenan

Department of Medicinal Chemistry and Molecular Pharmacology, Purdue University, West Lafayette, IN 47907, USA (S.E.E., P.Y.S., R.M.D.)

George E. Wahlen Veterans Affairs Medical Center and Departments of Psychiatry and Biology, University of Utah, Salt Lake City, UT 84148, USA (J.M.M.)

Downloaded from molpharm.aspetjournals.org at ASPET Journals on April 23, 2024

Copyright 2013 by the American Society for Pharmacology and Experimental Therapeutics.

Molecular Pharmacology Fast Forward. Published on June 20, 2013 as DOI: 10.1124/mol.113.087346
This article has not been copyedited and formatted. The final version may differ from this version.

Running Title: α6* nAChR activation enhances AMPA receptor function

Corresponding author:

Ryan M. Drenan

Purdue University

Department of Medicinal Chemistry and Molecular Pharmacology

575 Stadium Mall Dr.

West Lafayette, IN 47907

Phone: 765-494-1403

Fax: 765-494-1414

drenan@purdue.edu

# of text pages: 49

# of figures: 9

# of tables: 0

# of references: 60

# of words (Abstract): 250

# of words (Introduction): 724

# of words (Discussion): 1428

Downloaded from molpharm.aspetjournals.org at ASPET Journals on April 23, 2024

Molecular Pharmacology Fast Forward. Published on June 20, 2013 as DOI: 10.1124/mol.113.087346
This article has not been copyedited and formatted. The final version may differ from this version.

Non-standard abbreviations: nAChR, nicotinic acetylcholine receptor; DA, dopamine; VTA, ventral tegmental area; AMPA, 2-amino-3-(3-hydroxy-5-methyl-isoxazol-4-yl)propanoic acid; NMDA, N-methyl D-aspartic acid; EPSC, excitatory post-synaptic current; LTP, long-term potentiation; GABA, gamma aminobutyric acid; NE, norepinephrine; AP-5, D-2-amino-5-phosphonopentanoate; TTX, tetrodotoxin; CNQX, 6-cyano-7-nitroquinoxaline-2,3-dione; ACh, acetylcholine; ACSF, artificial cerebrospinal fluid; DIC, differential interference contrast; GFP, green fluorescent protein

Downloaded from molpharm.aspetjournals.org at ASPET Journals on April 23, 2024

Molecular Pharmacology Fast Forward. Published on June 20, 2013 as DOI: 10.1124/mol.113.087346
This article has not been copyedited and formatted. The final version may differ from this version.

Abstract

Tobacco addiction is a serious threat to public health in the United States and abroad, and development of new therapeutic approaches is a major priority. Nicotine activates and/or desensitizes nicotinic acetylcholine receptors (nAChRs) throughout the brain. nAChRs in ventral tegmental area (VTA) dopamine (DA) neurons are crucial for the rewarding and reinforcing properties of nicotine in rodents, suggesting that they may be key mediators of nicotine's action in humans. However, which nAChR subtype(s) that is/are sufficient to activate these neurons is unknown. To test the hypothesis that nAChRs containing α6 subunits are sufficient to activate VTA DA neurons, we studied mice expressing hypersensitive, gain-of-function α6 nAChRs (α6L9′S mice). In voltage clamp recordings in brain slices from adult mice, 100 nM nicotine was sufficient to elicit inward currents in VTA DA neurons via α6β2* nAChRs. In addition, we found that low concentrations of nicotine could act selectively through α6β2* nAChRs to enhance the function of 2-amino-3-(3-hydroxy-5-methyl-isoxazol-4-yl)propanoic acid (AMPA) receptors on the surface of these cells. In contrast, α6β2* activation did not enhance N-methyl D-aspartic acid (NMDA) receptor function. Finally, AMPAR function was not similarly enhanced in brain slices from α6L9′S mice lacking α4 nAChR subunits, suggesting that α4α6β2* nAChRs are important for enhancing AMPAR function in VTA DA neurons. Together, these data suggest that activation of α4α6β2* nAChRs in VTA DA neurons is sufficient to support the initiation of cellular changes that play a role in addiction to nicotine. α4α6β2* nAChRs may be a promising target for future smoking cessation pharmacotherapy.

Downloaded from molpharm.aspetjournals.org at ASPET Journals on April 23, 2024

Molecular Pharmacology Fast Forward. Published on June 20, 2013 as DOI: 10.1124/mol.113.087346
This article has not been copyedited and formatted. The final version may differ from this version.

Introduction

Compared to the 20th century, the number of deaths worldwide from tobacco use is estimated to be ten-fold greater at the completion of the 21st century – possibly as many as 1 billion lives lost (Peto and Lopez, 2001). Development of better smoking cessation therapies is, therefore, a major priority. Most current therapies seek to interfere with the action of nicotine, the primary psychoactive compound in cigarette smoke. Nicotine activates and/or desensitizes nicotinic acetylcholine receptors (nAChRs) found on neuronal axon terminals, dendrites, and somata (Picciotto et al., 2008; Pidoplichko et al., 1997). The mesolimbic dopamine (DA) pathway, including DA neurons in the ventral tegmental area (VTA) and their terminals in the nucleus accumbens (NAc), is a key brain circuit involved in nicotine addiction (Laviolette and van der Kooy, 2004). Nicotine acts through nAChRs in this pathway to stimulate DA neuron firing (Calabresi et al., 1989) and produce long-lasting increases in NAc DA release (Di Chiara and Imperato, 1988).

Long-lived enhancement of drug-induced DA release is thought to be mediated by changes in synaptic plasticity at VTA DA neurons (Kauer and Malenka, 2007; Wolf et al., 2004). This involves the abused drug causing enhanced excitability of VTA DA neurons and long-term potentiation (LTP) of excitatory inputs to these cells (Saal et al., 2003; Ungless et al., 2001). In particular, nicotine acts through VTA nAChRs on DA neuron somata, as well as presynaptic nAChRs, to depolarize these cells, facilitate N-methyl D-aspartic acid (NMDA) receptor activation, and enhance glutamate-induced excitatory post synaptic currents (EPSCs) (Gao et al., 2010; Jin et al., 2011; Mao et al., 2011; Saal et al., 2003). Understanding which proteins – including which nAChR

Downloaded from molpharm.aspetjournals.org at ASPET Journals on April 23, 2024

Molecular Pharmacology Fast Forward. Published on June 20, 2013 as DOI: 10.1124/mol.113.087346
This article has not been copyedited and formatted. The final version may differ from this version.

subtypes – mediate these effects could lead to new pharmacotherapy approaches designed to disrupt or reverse the addictive process at the molecular, cellular, or circuit level (Drenan and Lester, 2012).

Heteromeric nAChRs in brain are pentamers containing two or more β subunits (β2 and/or β4) and two or more α subunits (α2-α6) (Itier and Bertrand, 2001). "Auxiliary" subunits α5 or β3 do not contribute to formation of a functional binding site, but nevertheless exert powerful modulatory effects on nAChR function (Cui et al., 2003; Drenan et al., 2008b; Fowler et al., 2011). α4β2* (* = indicates nAChR pentamers that contain the indicated subunits, and may or may not contain other subunits as well) nAChRs are expressed in DAergic and GABAergic neurons in VTA (Nashmi et al., 2007), and activation of these receptors can produce increased firing of VTA DA neurons (Liu et al., 2012; Tapper et al., 2004) as well as increased GABA release onto these cells (Mansvelder et al., 2002). Homomeric α7 nAChRs expressed on glutamatergic axon terminals that synapse onto VTA neurons can enhance glutamatergic excitation of VTA neurons (Mansvelder and McGehee, 2000), thereby potentiating nicotine's direct action at α4β2* nAChRs on the soma of these cells (Mansvelder et al., 2002).

Interest in nAChRs containing α6 subunits is strong due to their high sensitivity to nicotine (Salminen et al., 2007), and their selective expression in DA and norepinephrine (NE)-producing cells (Champtiaux et al., 2002; Le Novere et al., 1996; Lena et al., 1999; Mackey et al., 2012). α6* nAChRs require β2 subunits for proper expression and function (Champtiaux et al., 2003; Grady et al., 2002; Salminen et al.,

Downloaded from molpharm.aspetjournals.org at ASPET Journals on April 23, 2024

Molecular Pharmacology Fast Forward. Published on June 20, 2013 as DOI: 10.1124/mol.113.087346
This article has not been copyedited and formatted. The final version may differ from this version.

2004). Tapper and colleagues demonstrated that activation of α4β2* nAChRs in VTA DA neurons induces prolonged depolarization of these cells, an effect that was sensitive to an α6* nAChR antagonist (Liu et al., 2012). Using a similar antagonist, Wu and colleagues reported that GABAergic transmission onto VTA DA neurons may be mediated by α6* nAChRs (Yang et al., 2011). These approaches relied on pharmacological blockade to discern the role of α6* nAChRs, and the results indicate that more experiments are needed to better understand α6* nAChRs in the VTA.

In the present study, we studied transgenic mice expressing α6 nAChR subunits with increased sensitivity to nicotine (Drenan et al., 2008a), which provided a complementary approach to pharmacological inactivation (Drenan and Lester, 2012). Using low concentrations of nicotine that moderately activate α6* nAChRs but do not activate (non-α6)* nAChRs, we tested the hypothesis that α6* nAChR activation in VTA DA neurons is sufficient to 1) elicit slow inward currents, and 2) enhance 2-amino-3-(3-hydroxy-5-methyl-isoxazol-4-yl)propanoic acid (AMPA) receptor function. Further, we also assessed whether α4 nAChR subunits were permissive in any or all of these measurements.

Downloaded from molpharm.aspetjournals.org at ASPET Journals on April 23, 2024

Molecular Pharmacology Fast Forward. Published on June 20, 2013 as DOI: 10.1124/mol.113.087346
This article has not been copyedited and formatted. The final version may differ from this version.

Materials and Methods

Mice

All experiments were conducted in accordance with the guidelines for care and use of animals provided by the Office of Laboratory Animal Welfare at the National Institutes of Health, and protocols were approved by the Institutional Animal Care and Use Committee at Purdue University. Mice were kept on a standard 12/12 light/dark cycle at 22°C and given food and water *ad libitum*. On postnatal day 21, mice were weaned and housed with same-sex littermates. Tail biopsies were taken for genotype analysis by PCR as previously described (Drenan et al., 2010).

α6L9′S mice were generated as described (Drenan et al., 2008a). Briefly, a mouse bacterial artificial chromosome (BAC) containing the *Chrna6* gene was obtained and an L9′S mutation was introduced by codon replacement using a BAC recombineering approach. Mutant BAC DNA was introduced into FVB/N embryos, which were then implanted into pseudopregnant Swiss-Webster surrogates. The BAC insertion site in the mouse genome is unknown. Founder animals were isolated and have been continuously back-crossed to C57BL/6 for > 12 generations. Over 90% of the α6L9′S strain genome is expected to contain C57BL/6 alleles, but FVB/N allelic DNA close to the insertion site is likely to remain in place in this strain. α6L9′S mice are thus transgenic and express mutant (L9′S) and WT α6 nAChR subunits (Cohen et al., 2012). α6* nAChR function is sensitized in these mice, producing a 10 to 100-fold leftward shift in concentration-response relationships involving α6* nAChRs, depending on the assay being used (Cohen et al., 2012; Drenan et al., 2010; Drenan et al., 2008a). We have

Downloaded from molpharm.aspetjournals.org at ASPET Journals on April 23, 2024

Molecular Pharmacology Fast Forward. Published on June 20, 2013 as DOI: 10.1124/mol.113.087346
This article has not been copyedited and formatted. The final version may differ from this version.

previously confirmed that α6* nAChRs in α6L9′S mice are not over-expressed or mis-expressed in ectopic brain locations (Drenan et al., 2010; Drenan et al., 2008a).

α6L9′S mice lacking α4 nAChR subunits were generated as previously described (Drenan et al., 2010). α4KO mice were a generous gift of Dr. Michael Marks (University of Colorado Boulder), and were produced by mating mice heterozygous for the α4KO allele. Briefly, α6L9′S mice, where the mutant allele is maintained in a heterozygous fashion, were crossed to homozygous α4KO mice to produce mice which are heterozygous for both the α6L9′S allele and the α4KO allele. These mice were subsequently crossed to homozygous α4KO mice to produce mice heterozygous for the α6L9′S allele and homozygous for the α4KO allele. α6GFP mice were generated as previously described (Mackey et al., 2012). To create α6GFP mice lacking α4 subunits, α4KO mice were crossed to α6GFP mice, generating α6GFP mice heterozygous for the α4KO allele. These mice were crossed again to mice homozygous for the α4KO allele, yielding α6GFP mice that were also homozygous for the α4KO allele. All groups of mice in this study contained approximately equal numbers of males and females.

Materials

All chemicals were from Sigma-Aldrich (St. Louis, MO). Sigma was also the source for the following compounds: atropine sulfate, (-)-nicotine tartrate, acetylcholine HCl, 2-amino-3-(3-hydroxy-5-methyl-isoxazol-4-yl)propanoic acid (AMPA), *N*-methyl-D-aspartic acid (NMDA), methyllycaconitine (MLA), SCH23390, and picrotoxin. Tocris Biosciences (Ellisville, MO) was the source of the following compounds: D-2-amino-5-phosphonopentanoate (AP-5), tetrodotoxin (TTX), 6-cyano-7-nitroquinoxaline-2,3-dione

Downloaded from molpharm.aspetjournals.org at ASPET Journals on April 23, 2024

Molecular Pharmacology Fast Forward. Published on June 20, 2013 as DOI: 10.1124/mol.113.087346
This article has not been copyedited and formatted. The final version may differ from this version.

(CNQX). α-conotoxin MII was synthesized by previously described methods (Azam et al., 2010).

Brain Slice Preparation for Electrophysiology

Brain slices were prepared as previously described (Engle et al., 2012). α6L9′S and non-Tg mice were genotyped at 21-28 days after birth. Mice were anesthetized with sodium pentobarbital (100 mg/kg; intraperitoneal, i.p.) followed by cardiac perfusion with oxygenated (95% O_2/5% CO_2), 4°C NMDG-recovery solution containing (in mM): 93 n-methyl D-glucamine, 2.5 KCl, 1.2 NaH_2PO_4, 30 $NaHCO_3$, 20 HEPES, 25 glucose, 5 Na^+ ascorbate, 2 thiourea, 3 Na^+ pyruvate, 10 $MgSO_4 \bullet 7H_2O$, 0.5 $CaCl_2 \bullet 2H_2O$ (300-310 mOsm, pH 7.3-7.4). Brains were removed and retained in 4°C NMDG-recovery solution for 1 min. Coronal slices (200 μm) were cut with a microslicer (DTK-Zero 1; Ted Pella, Redding, CA). Brain slices recovered for 12 min at 33°C in oxygenated NMDG-recovery solution, after which they were held until recording in HEPES holding solution containing (in mM): 92 NaCl, 2.5 KCl, 1.2 NaH_2PO_4, 30 $NaHCO_3$, 20 HEPES, 25 glucose, 5 Na^+ ascorbate, 2 thiourea, 3 Na^+ pyruvate, 2 $MgSO_4 \bullet 7H_2O$, 2 $CaCl_2 \bullet 2H_2O$ (300-310 mOsm, pH 7.3-7.4). Coordinates for recordings in VTA were approximately: (-3.5 mm from bregma, 4.0 to 4.5 mm from the surface, and 0.5 to 1.0 mm from the midline). In adult C57 mice, these coordinates correspond to nucleus accumbens lateral shell-projecting VTA neurons, which are expected to be ~96% tyrosine hydroxylase-positive (Lammel et al., 2008).

Patch Clamp Electrophysiology

Downloaded from molpharm.aspetjournals.org at ASPET Journals on April 23, 2024

Molecular Pharmacology Fast Forward. Published on June 20, 2013 as DOI: 10.1124/mol.113.087346
This article has not been copyedited and formatted. The final version may differ from this version.

Patch clamp electrophysiology was carried out as previously described (Engle et al., 2012). A single slice was transferred to a 0.8 ml recording chamber (Warner Instruments; Hamden, CT; RC-27L bath with PH-6D heated platform), and slices were superfused throughout the experiment with standard recording ACSF (1.5–2.0 ml/min) containing (in mM): 124 NaCl, 2.5 KCl, 1.2 NaH_2PO_4, 24 $NaHCO_3$, 12.5 glucose, 2 $MgSO_4 \cdot 7H_2O$, 2 $CaCl_2 \cdot 2H_2O$ (300-310 mOsm, pH 7.3-7.4). Cells were visualized with an upright microscope (FN-1; Nikon Instruments; Melville, NY) using infrared or visible differential interference contrast (DIC) optics. Patch electrodes were constructed from Kwik-Fil borosilicate glass capillary tubes (1B150F-4; World Precision Instruments, Inc.; Sarasota, FL) using a programmable microelectrode puller (P-97; Sutter Instrument Co.; Novato, CA). The electrodes had tip resistances of 4.5–8.0 MΩ when filled with internal pipette solution (pH adjusted to 7.25 with Tris base, osmolarity adjusted to 290 mOsm with sucrose). Two internal pipette solutions were used. The following solution was used when recording nicotine or ACh-evoked currents (bath application or puff-applied): 135 mM K^+ gluconate, 5 mM EGTA, 0.5 mM $CaCl_2$, 2 mM $MgCl_2$, 10 mM HEPES, 2 mM Mg-ATP, and 0.1 mM GTP. The following solution was used when recording AMPA- or NMDA-evoked currents: 117 mM $CsCH_3SO_3$, 20 mM HEPES, 0.4 mM EGTA, 2.8 mM NaCl, 5 mM TEA-Cl, 2.5 mM MgATP, 100 μM spermine, and 0.25 mM MgGTP (pH 7.25 with tris base). Whole-cell recordings were taken at 32°C with an Axopatch 200B amplifier, a 16-bit Digidata 1440A A/D converter, and pCLAMP 10.3 software (all Molecular Devices; Sunnyvale, CA). Data were sampled at 5 kHz and low-pass filtered at 1 kHz. The junction potential between the patch pipette and the bath solution was nulled immediately prior to gigaseal formation. Series resistance was uncompensated.

Downloaded from molpharm.aspetjournals.org at ASPET Journals on April 23, 2024

Molecular Pharmacology Fast Forward. Published on June 20, 2013 as DOI: 10.1124/mol.113.087346
This article has not been copyedited and formatted. The final version may differ from this version.

DA neurons in VTA were identified according to previously published methods (Drenan et al., 2008a; Nashmi et al., 2007; Wooltorton et al., 2003). We avoided recording from neurons on the slice surface and neurons deep in the slice that were difficult to visualize. Briefly, DA neurons were identified via several electrophysiological characteristics: 1) broad spike width ($\geq$ 2 msec), 2) slow spontaneous firing (< 5 Hz), and 3) expression of hyperpolarization-activated cation current (I_h). To examine the function of somatic ligand-gated ion channels, agonists were locally applied using a Picospritzer III (General Valve; Fairfield, NJ) as previously described (Engle et al., 2012). Atropine (1 μM) was present in the bath solution when administering ACh to avoid activation of muscarinic receptors. A drug-filled micropipette, identical to a typical recording pipette, was mounted onto a single-dimension piezoelectric translator (PA-100/12; piezosystem jena, Inc.), which was fixed to a micromanipulator (Sutter Instruments). Between drug applications, the drug-filled pipette was maintained $\geq$ 100 μm from the recorded cell. To apply drugs to the recorded cell, pClamp software triggered the piezoelectric translator to advance the drug-filled pipette to a predetermined position adjacent to the recorded cell (20 - 40 μm from the cell), drug was applied to the cell using a 250 msec pressure (12 psi) ejection, and the piezoelectric translator subsequently retracted the drug-filled pipette. This setup allowed for better reproducibility and reduced receptor desensitization compared with manual control of the drug-filled pipette (Engle et al., 2012). The first application to a cell was typically with the drug-filled tip ~40 μm from the cell, and we subsequently moved the position of the drug-filled pipette closer to the cell to achieve a more rapid response. Responses to AMPA were deemed acceptable based on two criteria: 1) the

Downloaded from molpharm.aspetjournals.org at ASPET Journals on April 23, 2024

Molecular Pharmacology Fast Forward. Published on June 20, 2013 as DOI: 10.1124/mol.113.087346
This article has not been copyedited and formatted. The final version may differ from this version.

pressure application caused slight to modest cell movement, and 2) the seal parameters remained stable for multiple responses. Under these conditions, the 10-90% rise time for AMPA application was 222 ± 17 msec. Faster rise times and excessive cell movement were commonly associated with loss of a stable seal. Responses were much slower (10-90% rise time was 546 ± 75 msec) when the cell did not move during the application.

Single-cell RT-PCR

These methods were adapted from (Zhao-Shea et al., 2011). VTA neurons were studied using K^+ gluconate-based internal solution (see recipe above) made with DEPC-treated water. After whole-cell recording, the recorded cell was aspirated into the pipette, under visual control, with gentle negative pressure. Input resistance was monitored during aspiration. Successful PCR reactions were typically only attained when a seal resistance of > 1 GΩ was maintained after aspiration. Cellular contents were expelled into 75% ethanol, and RNA was precipitated and isolated by centrifugation at 4°C. cDNA was formed from RNA via reverse transcription (Sensicript RT, Qiagen) using oligo-dT primers, and a nested PCR strategy was subsequently used to detect target mRNA species. In round #1 of nested PCR, TH and GAPDH cDNA was amplified (1 cycle: 94°C 2 min; 20 cycles: 94°C 1 min, 56°C 1 min, and 72°C 1.5 min; 1 cycle: 72°C 10 min) with the following primers: TH_F (CAGTGATGCCAAGGACAAGC), TH_R2 (GAGAAGGGGCTGGGAACTTT), GAPDH_F2 (AACTTTGGCATTGTGGAAGG), and GAPDH_R2 (CCCTGTTGCTGTAGCCGTAT). Subsequently, TH and GAPDH signals were further amplified (1 cycle: 94°C 2 min; 36 cycles: 94°C 1 min, 56°C 1 min, 72°C 1.5 min; 1 cycle: 72°C 10 min) in round #2 with

Downloaded from molpharm.aspetjournals.org at ASPET Journals on April 23, 2024

Molecular Pharmacology Fast Forward. Published on June 20, 2013 as DOI: 10.1124/mol.113.087346
This article has not been copyedited and formatted. The final version may differ from this version.

the following primers: TH_F, TH_R1 (CCT GTG GGT GGT ACC CTA TG), GAPDH_F1 (GTG TTC CTA CCC CCA ATG TG), and GAPDH_R1 (GGT CCT CAG TGT AGC CCA AG). PCR primers were synthesized by IDT (Coralville, IA). Final PCR products were detected by electrophoresis in 1.6% agarose gels with ethidium bromide staining.

Immunohistochemistry and Confocal Microscopy

Transgenic mice expressing α6* nAChR subunits fused in-frame with green fluorescent protein (GFP) (α6GFP mice; *n* = 3), along with α6GFP mice homozygous for the α4KO allele, were anesthetized with sodium pentobarbital (100 mg/kg; i.p.) and transcardially perfused with 15 ml of ice-cold PBS followed by 25 ml of ice-cold 4% paraformaldehyde (PFA) in PBS. Brains were removed and postfixed for 2 hr at 4°C. Coronal sections (50 µm) were cut on a microslicer and collected into PBS. Sections were permeabilized (20 mM HEPES, pH 7.4, 0.5% Triton X-100, 50 mM NaCl, 3 mM $MgCl_2$, 300mM sucrose) for 1 hr at 4°C, blocked (0.1% Triton X-100, 5% donkey serum in TBS) for 1 hr at room temperature (RT), and incubated overnight at 4°C in solutions containing primary antibodies (diluted in 0.1% Triton X-100, 5% donkey serum in TBS). Sections were stained with rabbit anti-GFP (A11122; Invitrogen: Carlsbad, CA) primary antibodies with a final dilution of 1:500. Sections were washed three times for 10 min each in TBST (0.1% Triton X-100 in TBS) followed by incubation at RT for 1 hr with secondary antibodies (diluted in 0.1% Triton X-100, 5% donkey serum in TBS): 1:1000 goat anti-rabbit Alexa 488 (A11008; Invitrogen). Sections were then washed three times in TBST for 10 min each. Sections were stained with the nuclear dye, Qnuclear (1:1000; Qnuclear Deep Red Stain; Q10363, Invitrogen) in PBS for 20 min at RT followed by three 5 min washes in PBS. All sections were mounted on slides and coverslipped with

Downloaded from molpharm.aspetjournals.org at ASPET Journals on April 23, 2024

Molecular Pharmacology Fast Forward. Published on June 20, 2013 as DOI: 10.1124/mol.113.087346
This article has not been copyedited and formatted. The final version may differ from this version.

Vectashield (Vector Laboratories), then imaged with a Nikon (Nikon Instruments) A1 laser-scanning confocal microscope system. Nikon Plan Apo 10X air and 60X oil objectives were used. Alexa 488 was excited with an argon laser at 488 nm. VTA DA neurons were imaged at 60X, and mean pixel intensity per cell was measured for > 100 cells in both α6GFP and α6GFPα4KO slices.

Statistics and Data Analysis

Statistical analysis was performed with GraphPad Prism 6 software. Data are reported as mean ± SEM. To determine whether data sets were normally distributed, all data sets were subjected to a D'Agostino & Pearson omnibus normality test. Only when all data sets to be compared passed this normality test (α level = 0.05) were parametric statistical tests used. For data sets that were either 1) not normally distributed or 2) not large enough for a normality test, statistical significance ($p < 0.05$) was assessed with non-parametric tests: a Mann-Whitney test was used for comparisons between two groups, and a Kruskall-Wallis (non-parametric 1-way ANOVA) test followed by a Dunn's post-hoc test was used for comparisons between three or more groups. Concentration response curve data was fitted to the Hill equation. Error bars for plotted EC_{50} values indicate 95% confidence interval.

Downloaded from molpharm.aspetjournals.org at ASPET Journals on April 23, 2024

Molecular Pharmacology Fast Forward. Published on June 20, 2013 as DOI: 10.1124/mol.113.087346
This article has not been copyedited and formatted. The final version may differ from this version.

Results

To study VTA DA neurons in adult (≥ 60 days old) mice, we prepared coronal slices and recorded from VTA cells residing in the lateral aspect of the VTA. Although the VTA is emerging as a heterogeneous structure (Lammel et al., 2011), 96.3% of neurons in this area test positive for tyrosine hydroxylase (TH) expression in adult C57 mice, and these cells exhibit I_h currents (Lammel et al., 2011). VTA neurons in this study typically fired spontaneous (Fig. 1A), wide (Fig. 1B; width = ~2-5 msec) action potentials. Hyperpolarizing current injections induced "sag" responses in the transmembrane voltage record (Fig. 1A, I = -120 pA), and these cells exhibited inward currents in response to hyperpolarizing voltage steps (I_h currents; Fig. 1C). To provide further confirmation that these neurons are DAergic, we conducted single-cell reverse transcriptase PCR reactions from a subset of recorded neurons. All recorded neurons (n = 5) in lateral VTA (see Materials and Methods for coordinates) with a PCR signal for GAPDH were also positive for TH mRNA (Fig. 1D), and all of these TH(+) cells exhibited electrophysiological features as shown above (Fig. 1, A-C). Based on these results and supporting studies in the literature (Lammel et al., 2008; Lammel et al., 2011; Zhang et al., 2010), we proceeded with reasonable confidence that cells with these characteristics, and in this lateral part of the VTA, were DAergic neurons.

First, we tested the hypothesis that activation of α6* nAChRs is sufficient to elicit inward currents in VTA DA neurons by recording from VTA DA neurons from adult α6L9′S and non-transgenic (non-Tg) littermate mice. Whole-cell voltage-clamp recordings from VTA DA neurons were established using a K^+ gluconate-based internal recording solution, and an inhibitor cocktail containing CNQX (10 μM), picrotoxin (75 μM), and TTX (0.5

Downloaded from molpharm.aspetjournals.org at ASPET Journals on April 23, 2024

Molecular Pharmacology Fast Forward. Published on June 20, 2013 as DOI: 10.1124/mol.113.087346
This article has not been copyedited and formatted. The final version may differ from this version.

μM) was bath-applied to the cell to eliminate most external influences on membrane potential. We measured inward currents in response to a 10-min bath exposure to nicotine. We previously reported that brief (250 msec), puff-application of 100 nM nicotine elicited small (~10 pA) inward currents (Drenan et al., 2008a). We reasoned that sustained exposure of VTA DA neurons to 100 nM nicotine could be sufficient to provide prolonged activation of these cells. Nicotine (100 nM) elicited a significant inward current in α6L9′S VTA DA neurons (Fig. 2, A and B; mean change in holding current value relative to pre-nicotine baseline = -18.0 ± 3.0 pA). Co-application of α-conotoxin MII (αCtxMII; 100 nM) with nicotine (100 nM) eliminated these inward currents (Fig. 2, A, B and E; mean change in holding current value relative to pre-nicotine baseline = -2.7 ± 4.1 pA; $p < 0.05$, Mann-Whitney test), suggesting that α6* nAChRs mediate inward currents in response to 100 nM nicotine. To determine whether responses to 100 nM nicotine were selective for α6* nAChRs in α6L9′S slices, 100 nM nicotine was applied to VTA DA neurons from non-Tg littermate slices. Nicotine (100 nM) only slightly increased inward currents in non-Tg littermate VTA DA neurons in this assay (Fig. 2, C and E; mean change in holding current value relative to pre-nicotine baseline = -3.1 + 0.8 pA), but the same concentration of nicotine significantly increased inward currents in α6L9′S neurons (Fig. 2E; $p < 0.05$, Mann-Whitney test). αCtxMII did not alter this response in non-Tg littermate cells (Fig. 2E). As a positive control, we applied 300 nM nicotine to non-Tg VTA DA neurons. This concentration was sufficient to moderately increase inward currents in these cells (Fig. 2, D and E; mean change in holding current value relative to pre-nicotine baseline = -8.7 ± 2.2 pA), consistent with a previous report (Liu et al., 2012). αCtxMII did not block these

Downloaded from molpharm.aspetjournals.org at ASPET Journals on April 23, 2024

Molecular Pharmacology Fast Forward. Published on June 20, 2013 as DOI: 10.1124/mol.113.087346
This article has not been copyedited and formatted. The final version may differ from this version.

responses (Fig. 2, D and E; mean change in holding current value relative to pre-nicotine baseline = -7.0 $\pm$ 1.0 pA), presumably because responses in non-Tg cells are mediated by both α6* and non-α6* ($\alpha4\beta2$) nAChRs. Together, these results demonstrate that selective activation of α6* nAChRs is sufficient to increase inward currents in VTA DA neurons. Application of 100 nM nicotine to α6L9′S slices was used in subsequent experiments to study the effects of selectively activating α6* nAChRs.

The initial exposure of brain cells to smoking-relevant concentrations of nicotine results in activation of high-sensitivity nAChRs, including those on VTA DA neurons (Calabresi et al., 1989). This exposure to nicotine leads to up-regulation of AMPA receptor (AMPAR) function in these cells (Saal et al., 2003), which could support behavioral changes that lead to nicotine dependence. Because high-sensitivity nAChRs are expressed on 1) VTA DA neurons, 2) terminals from GABA neurons that synapse onto VTA DA neurons, and 3) other glutamatergic fibers, it is not known whether activation of nAChRs specifically on VTA DA neurons can lead to increased AMPAR function. We previously demonstrated that α6* nAChRs are expressed only in DA neurons in VTA (Mackey et al., 2012). We hypothesized that selective activation of α6* nAChRs in VTA, which should stimulate DA neurons but not other VTA nAChRs (such as those on GABA or glutamatergic terminals) (Drenan et al., 2008a) is sufficient to enhance AMPAR function in these cells.

To measure AMPAR function on the cell surface, we applied AMPA to VTA DA neurons using a drug-filled pipette (Kobayashi et al., 2009; Li et al., 2008; Sanchez et al., 2010) that was positioned using a piezoelectric translator (Engle et al., 2012). A cell was voltage clamped and a stable recording was established. The drug-filled pipette

Downloaded from molpharm.aspetjournals.org at ASPET Journals on April 23, 2024

Molecular Pharmacology Fast Forward. Published on June 20, 2013 as DOI: 10.1124/mol.113.087346
This article has not been copyedited and formatted. The final version may differ from this version.

remained stationary above/outside the slice until our recording software delivered an analog signal to the piezoelectric translator, triggering movement of the pipette to a pre-determined position ~20-40 μm from the recorded cell. A digital TTL pulse (5V, 250 msec duration) activated the picospritzer, resulting in drug delivery to the recorded cell. After the TTL pulse, the piezoelectric translator withdrew the drug-filled pipette. This procedure is summarized in schematic form in Fig. 3A. Fig. 3B shows a representative record of the movement of the piezoelectric translator, the TTL pulse, and a response to 100 μM AMPA in a VTA DA neuron.

To test the hypothesis that selective activation of α6* nAChRs is sufficient to enhance AMPAR function, we prepared coronal slices from α6L9′S mice and their non-Tg littermates. Slices were cut and allowed to recover for 60 min, followed by exposure of the slices to 100 nM nicotine (or a control solution containing no nicotine) for 60 min similar to previous studies (Jin et al., 2011; Mao et al., 2011) (Fig. 4A). After a washout period (≥ 60 min), whole-cell recordings were established in VTA DA neurons using a Cs-methanesulfonate-based internal solution. AMPA currents were evoked at holding potentials of -60 mV, 0 mV, and +40 mV. Whereas nicotine (100 nM) exposure did not alter AMPAR function in non-Tg VTA DA neurons, this treatment was sufficient to robustly increase AMPA-evoked currents in α6L9′S VTA DA neurons (Fig. 4B). Mean AMPA-evoked current amplitude was not altered by nicotine (100 nM) at -60 mV, 0 mV, or +40 mV in non-Tg littermates (Fig. 4C). In contrast, there was a significant increase in AMPA-evoked current amplitude at -60 mV and +40 mV in α6L9′S neurons (Fig. 4D; -60 mV = -173.5 ± 29.4 pA (control), -358.4 ± 48.5 pA (100 nM nicotine), p = 0.004, Mann-Whitney test; +40 mV = 82.2 ± 14.3 pA (control), 167.1 ± 23.5 pA (100 nM

Downloaded from molpharm.aspetjournals.org at ASPET Journals on April 23, 2024

Molecular Pharmacology Fast Forward. Published on June 20, 2013 as DOI: 10.1124/mol.113.087346
This article has not been copyedited and formatted. The final version may differ from this version.

nicotine), p = 0.0045, Mann-Whitney test). As a positive control, we incubated non-Tg slices in a higher concentration of nicotine (500 nM). This treatment led to a significant increase in AMPA-evoked currents at a holding potential of -60 mV (Fig. 4, B and C; -60 mV = -184.2 $\pm$ 18.3 pA (control), -283.4 $\pm$ 35.8 pA (500 nM nicotine), p = 0.0487, unpaired t test), consistent with previously published experiments with VTA DA neurons in slices (Jin et al., 2011).

Next, we sought to determine whether enhanced AMPA-evoked currents in α6L9′S slices treated with nicotine (100 nM) was due to a change in the efficacy vs. the potency of AMPA. First, we constructed an AMPA concentration-response curve to confirm that changes in AMPA-evoked currents between non-Tg and α6L9′S slices were not due to differences in initial AMPAR sensitivity. Multiple concentrations of AMPA were applied to α6L9′S and non-Tg neurons, and the data were fitted to the Hill equation (non-Tg: R^2 = 0.9467; α6L9′S: R^2 = 0.9819). There was no substantial difference in AMPA EC_{50} in α6L9′S VTA DA neurons compared to non-Tg neurons (Fig. 4E; EC_{50} = 174 μM (non-Tg); EC_{50} = 182 μM (α6L9′S). Fig. 4E plots these EC_{50} values along with their respective 95% confidence intervals. Similarly, we constructed a concentration-response curve for AMPA-evoked currents in α6L9′S slices exposed to nicotine. AMPA at a range of concentrations was applied to cells in slices exposed to nicotine, and the data were fitted to the Hill equation (α6L9′S nicotine: R^2 = 0.9942). The EC_{50} for AMPA-evoked currents in nicotine-exposed α6L9′S slices was shifted to the left compared to α6L9′S slices not exposed to nicotine (Fig. 4F; EC_{50} = 37 μM), suggesting an increase in the sensitivity of AMPARs to AMPA.

Downloaded from molpharm.aspetjournals.org at ASPET Journals on April 23, 2024

Molecular Pharmacology Fast Forward. Published on June 20, 2013 as DOI: 10.1124/mol.113.087346
This article has not been copyedited and formatted. The final version may differ from this version.

Next, we studied the time-dependence for enhancement of AMPAR function in VTA DA neurons. As with previous experiments, slices were cut and allowed to recover for 60 min. Following this, we compared AMPA-evoked current amplitudes from neurons treated in four different ways: 1) incubated for 60 min in a control solution without nicotine followed by a washout period of 60 – 240 min prior to recording, 2) incubated for 60 min in nicotine (100 nM) followed by a washout period of 60 – 240 min prior to recording, 3) incubated for 10 min in nicotine (100 nM) followed by a washout period of 60 – 240 min prior to recording, and 4) incubated for 60 min in nicotine (100 nM) followed by a washout period of greater than 240 min prior to recording (Fig. 5A). Exposure of α6L9′S slices to 100 nM nicotine for 10 min was insufficient to augment AMPA-evoked currents above control levels (Fig. 5, B and C; control incubation/washout 60-240 min = -173.5 ± 29.4 pA, 10 min nicotine incubation/washout 60-240 min = -213.5 ± 27.9 pA). However, a 60 min exposure to nicotine was sufficient to augment AMPA-evoked currents over control (Fig. 5, B and C; 60 min nicotine incubation/washout 60-240 min = -351.1 $\underline{+}$ 64.9 pA; Kruskall-Wallis test, $p < 0.05$). The effect of a 60 min nicotine exposure was prolonged, as AMPA-evoked currents were still enhanced after a washout period of > 240 min (Fig. 5, B and C; 60 min nicotine incubation/washout 60-240 min = -411.4 $\underline{+}$ 75.5 pA; Kruskall-Wallis test, $p < 0.05$).

To better understand the mechanism within VTA DA neurons that leads to enhanced AMPA-evoked currents, we pre-treated α6L9′S slices for 10 min with several pharmacological agents prior to 60 min nicotine (100 nM) exposure, washout, and subsequent AMPA-evoked current measurements (Fig. 6A). Pretreatment of slices with αCtxMII eliminated the enhanced AMPA-evoked currents seen in α6L9′S slices

Downloaded from molpharm.aspetjournals.org at ASPET Journals on April 23, 2024

Molecular Pharmacology Fast Forward. Published on June 20, 2013 as DOI: 10.1124/mol.113.087346
This article has not been copyedited and formatted. The final version may differ from this version.

exposed to a control pre-treatment prior to nicotine exposure (Fig.6, B and C; control = -173.5 ± 29.4 pA, nicotine = -358.4 ± 48.5 pA, MII = -221.5 ± 45.8 pA; Kruskall-Wallis test, $p < 0.05$). Similarly, blockade of NMDA receptors with D-2-amino-5-phosphonopentanoate (AP-5; 10 μM) prior to nicotine treatment eliminated enhanced AMPA-evoked currents (Fig. 6, B and C; AP-5 = -194.4 ± 32.9 pA; Kruskall-Wallis test, $p < 0.05$). Previous studies indicate that DA D1/D5 receptors in VTA may play a role in altered synaptic plasticity following exposure to drugs of abuse (Gao and Wolf, 2007; Mao et al., 2011). Blockade of DA D1/D5 receptors with SCH23390 (10 μM) did not appear to substantially reduce nicotine-mediated enhancement in AMPA-evoked currents (Fig. 6, B and C; SCH = -325.0± 44.7 pA), but a Kruskall-Wallis test comparing AMPA-evoked currents from α6L9′S SCH23390-treated slices and untreated control α6L9′S slices did not reveal a statistical difference. Several previous reports indicate that homomeric α7 nAChRs play a role in nicotine-elicited AMPAR up-regulation (Gao et al., 2010; Jin et al., 2011). However, pre-treatment of slices with methyllycaconitine (MLA; 10 nM) did not reduce nicotine-elicited AMPAR up-regulation in α6L9′S VTA DA neurons (Fig. 6, B and C; MLA = -497.8 ± 119.8 pA; Kruskall-Wallis test, $p < 0.05$).

Elimination of α4 nAChR subunits via gene knockout has been shown to significantly reduce α6* nAChR function in synaptosomal DA release experiments (Drenan et al., 2010; Salminen et al., 2007; Salminen et al., 2004), direct assays of striatal nAChR function in brain slices (Drenan et al., 2010), and in behavioral experiments (Drenan et al., 2010). To test the hypothesis that α4 nAChR subunits are important for α6* nAChR-mediated enhancement of AMPAR function in VTA DA neurons, we crossed α6L9′S mice with α4KO animals to eliminate α4 nAChR subunits while still retaining

Downloaded from molpharm.aspetjournals.org at ASPET Journals on April 23, 2024

Molecular Pharmacology Fast Forward. Published on June 20, 2013 as DOI: 10.1124/mol.113.087346
This article has not been copyedited and formatted. The final version may differ from this version.

gain-of-function α6 subunits (Drenan et al., 2010). Slice treatment in this experiment (Fig. 7A) was identical to experiments reported in Fig. 4. Whereas nicotine (100 nM) treatment of α6L9′S slices leads to enhanced AMPAR function, identical treatment of slices from α6L9′S mice lacking α4 subunits did not increase AMPA-evoked currents (Fig. 7, B and C; α6L9′S: control = -173.5 ± 29.4 pA, nicotine = -358.4 ± 48.5 pA; α6L9′Sα4KO: control = -205.9 ± 23.3 pA, nicotine = -280.3 ± 45.3 pA; Kruskall-Wallis test, $p < 0.05$ for α6L9′S control vs. nicotine and $p > 0.05$ for α6L9′Sα4KO control vs. nicotine). To determine whether these results were due to reduced α6 expression and/or function, we performed a series of controls using α4KO animals. First, we crossed α4KO mice with transgenic mice expressing α6 subunits fused with green fluorescent protein (GFP; Fig. 8A). This manipulation results in the production of only (non-α4)α6β2* nAChRs (Fig. 8B). We used anti-GFP immunohistochemistry and confocal microscopy, as previously described in these mice (Mackey et al., 2012), to quantify α6* nAChR expression in VTA neurons in α6GFP mice and α6GFP mice crossed to α4KO mice. We found a small but significant reduction in α6GFP expression in VTA neurons in α6GFP mice lacking α4 subunits compared with α6GFP with intact α4 nAChR subunit expression (Fig. 8C; α4WT = 17921 ± 698 AU, α4KO = 14507 ± 816 AU, $p = 0.0011$, Mann-Whitney test). Next, we measured α6* nAChR function directly by comparing nicotine- and acetylcholine (ACh)-evoked currents in α6L9′S mice and α6L9′S mice lacking α4 subunits (Fig. 8D). In contrast to ACh-evoked responses in α6L9′S VTA DA neurons with intact α4 subunits, responses from VTA DA neurons in α6L9′S slices lacking α4 subunits were smaller (Fig. 8E). Inward current amplitudes

Downloaded from molpharm.aspetjournals.org at ASPET Journals on April 23, 2024

Molecular Pharmacology Fast Forward. Published on June 20, 2013 as DOI: 10.1124/mol.113.087346
This article has not been copyedited and formatted. The final version may differ from this version.

following puff-application of both 1μM and 100 μM ACh were smaller in α6L9′Sα4KO neurons relative to α6L9′S neurons (Fig. 8, E and F; α4WT 1 μM ACh = -171 ± 30.3 pA, α4KO 1 μM ACh = -57.8 ± 21.8 pA, α4KO 100 μM ACh = -77.6 ± 20.2 pA). Similarly, α6L9′S VTA DA neurons lacking α4 subunits were less sensitive to nicotine compared to α6L9′S cells expressing α4 subunits (Fig. 8G). Whereas 1 μM nicotine evoked large inward currents in α6L9′S VTA DA neurons that express α4 subunits, 30 μM nicotine was required to elicit inward currents of the same amplitude in α6L9′S slices lacking α4 subunits (Fig. 8, G and H; α4WT 1 μM nicotine = -198.4 ± 25.8 pA, α4KO 1 μM nicotine = -58.3 ± 11.5 pA, α4KO 30 μM nicotine = -189.6 ± 45.4 pA). Together, these experiments suggest that activation of α4α6β2* nAChRs are responsible for enhanced AMPA-evoked currents in α6L9′S VTA DA neurons.

Finally, we tested whether nicotine (100 nM), acting through α6* nAChRs, can increase or decrease NMDA receptor function on the surface of VTA DA neurons (Ungless et al., 2001). Whole-cell voltage-clamp recordings were established in VTA DA neurons, and NMDA currents were evoked via puff-application of NMDA at a holding potential of +40 mV. Incubation of α6L9′S and non-Tg slices in nicotine (100 nM) for 60 min (Fig. 9A) did not result in changes in NMDA-evoked currents relative to control treatments (Fig. 9, B and C; control: non-Tg = 167.8 ± 17.8 pA, α6L9′S = 172.8 ± 32.6 pA; nicotine: non-Tg = 185.2 ± 28.5 pA, α6L9′S = 167.3 ± 18.7 pA; Kruskall-Wallis test, p = 0.7893). These results suggest that, although NMDA activation is required for up-regulation of AMPAR function on VTA DA neurons (Fig. 6), activation of nAChRs does not significantly alter NMDA function after 60 min of exposure to nicotine.

Downloaded from molpharm.aspetjournals.org at ASPET Journals on April 23, 2024

Molecular Pharmacology Fast Forward. Published on June 20, 2013 as DOI: 10.1124/mol.113.087346
This article has not been copyedited and formatted. The final version may differ from this version.

Discussion

Our recordings in isolated brain slices demonstrate that selective activation of α6β2* nAChRs by nicotine is sufficient to increase slow inward currents in VTA DA neurons (Fig. 2) and enhance the function of AMPARs (Fig. 4). Our finding that greater than 10 min of exposure to nicotine is required to enhance AMPAR function (Fig. 5) suggests that multiple signal transduction events and/or ionic conductances are involved. Whereas α7 nAChR activation is not required (Fig. 6), NMDA receptor activation is necessary for α6β2*-mediated enhanced AMPAR function (Fig. 6). Interestingly, α6β2*-mediated AMPAR enhancement requires midbrain α4 nAChR subunits (Fig. 7), suggesting that pentamers containing both α4 and α6 subunits are responsible. These data, together with previous findings showing that α6β2* nAChRs are selectively expressed in DA neurons within the VTA (Mackey et al., 2012), suggest that nicotine can act exclusively in a postsynaptic manner on VTA DA neurons to sensitize these cells to excitatory input.

VTA DA neuron activation by α6β2 nAChRs*

Understanding which nAChR subtypes are necessary and sufficient to mediate nicotine's complex action on VTA neurons is a challenge (Drenan and Lester, 2012), and our data provide new information. We show that nicotine-elicited activation of somatodendritic α6β2* nAChRs in VTA DA neurons is sufficient to stimulate an inward conductance that could, under physiological conditions, support prolonged depolarization of these cells (Fig. 2). β2* nAChRs are absolutely required for nicotine-induced increases in VTA DA neuron firing (Maskos et al., 2005; Picciotto et al., 1998),

Downloaded from molpharm.aspetjournals.org at ASPET Journals on April 23, 2024

Molecular Pharmacology Fast Forward. Published on June 20, 2013 as DOI: 10.1124/mol.113.087346
This article has not been copyedited and formatted. The final version may differ from this version.

and Tapper and colleagues recently reported that activation of α4β2* nAChRs in VTA DA neurons by smoking-relevant concentrations of nicotine can support depolarization and action potential firing (Liu et al., 2012). These actions were sensitive to a α6β2* nAChR antagonist, implicating α4α6β2* nAChRs. This report is consistent with our study, which suggests that α6β2* nAChR activation can increase inward currents in VTA DA neurons (Fig. 2). Other reports studying the role of VTA α6β2* nAChRs in nicotine self-administration (Gotti et al., 2010; Pons et al., 2008) and DA release (Gotti et al., 2010) support the data we present here. Furthermore, our experiments employing puff-application of nicotine and ACh in α6L9′S and α6L9′Sα4KO brain slices (Fig. 8) provide evidence that α4 subunits play an important role in α6-mediated neuronal activation. In VTA, α4β2* nAChRs are found in DAergic neurons and in GABAergic neurons and/or terminals (Nashmi et al., 2007). Nicotine may act through VTA α4β2* nAChRs via two mechanisms: direct activation at α4β2* nAChRs on DA neurons, and/or desensitization of α4β2* nAChRs in GABAergic neurons leading to DA neuron disinhibition (Mansvelder et al., 2002; Nashmi et al., 2007). Because α6* nAChRs are restricted to DAergic cells in VTA (Mackey et al., 2012), our results suggest that direct action by nicotine on somatodendritic α6* nAChRs may be sufficient to depolarize these cells. In human brain, there may be redundant mechanisms in the VTA that allow nicotine to activate the mesolimbic DA system. Although our previous work indicates no evidence for overexpression of α6β2* nAChRs (Drenan et al., 2010), the TM2 pore-lining mutation used to sensitize these receptors may alter their pharmacological properties (Labarca et al., 1995; Revah et al., 1991). Future studies using restricted expression of α4α6L9′Sβ2* nAChRs via concatamers (Kuryatov and

Downloaded from molpharm.aspetjournals.org at ASPET Journals on April 23, 2024

Molecular Pharmacology Fast Forward. Published on June 20, 2013 as DOI: 10.1124/mol.113.087346
This article has not been copyedited and formatted. The final version may differ from this version.

Lindstrom, 2011) will be useful in exploring the latter possibility, while development of α6β2*-selective ligands will be useful in addressing the importance of the former possibility.

Nicotine-induced changes in AMPAR function

To our knowledge, this study is the first to implicate α6β2* nAChRs in nicotine-induced changes in AMPAR function in VTA DA neurons. A single exposure to nicotine or other drugs of abuse enhances AMPAR-mediated excitatory postsynaptic currents in VTA DA neurons (Saal et al., 2003), which strongly suggests long-term potentiation of excitatory inputs to these cells (Luscher and Malenka, 2011; Mansvelder and McGehee, 2000; Ungless et al., 2001). Subsequent studies addressing which nAChR subtypes mediate this effect are not completely consistent. In slice experiments, McGehee and colleagues report that β2* nAChRs (but not α7 nAChRs) are necessary for increased AMPAR function in synapses following nicotine exposure (Mao et al., 2011), whereas in studies with animals injected with nicotine prior to slice preparation, Wu and colleagues suggest that nicotine-elicited increases in AMPAR function can proceed either through β2* or α7 nAChRs (Gao et al., 2010; Jin et al., 2011). Our results using naïve or nicotine-exposed slices from adult non-Tg or α6L9′S mice are more consistent with the former, as we find no necessary role for α7 nAChRs in AMPAR functional enhancement (Fig. 6). As in any comparison between scientific studies, differences in experimental details may account for disparate results. Similar to previous approaches (Kobayashi et al., 2009; Sanchez et al., 2010; Ungless et al., 2001), our experiments used direct application of AMPA to VTA cell bodies. Thus, our results likely include a contribution from non-synaptic AMPAR pools on the plasma membrane of VTA DA neurons.

Downloaded from molpharm.aspetjournals.org at ASPET Journals on April 23, 2024

Molecular Pharmacology Fast Forward. Published on June 20, 2013 as DOI: 10.1124/mol.113.087346
This article has not been copyedited and formatted. The final version may differ from this version.

However, the fact that incubating non-Tg slices in 500 nM nicotine led to a significant increase in whole-cell AMPA-evoked currents gave us confidence that we are studying a similar increase in AMPAR function compared to the phenomenon seen in other reports that utilized electrically-evoked EPSCs as an endpoint. Future studies probing LTP in α6L9′S neurons will address the relative role of synaptic versus non-synaptic AMPAR pools in the response to nicotine.

In VTA DA neurons, changes in both AMPAR *distribution* and/or *composition* are proposed to occur following exposure to nicotine and other drugs of abuse. Several reports suggest that drug exposure (including nicotine) leads to signal transduction events that promote exchange of Ca^{2+}-impermeable AMPARs containing GluR2 subunits for high-conductance, Ca^{2+}-permeable AMPARs lacking GluR2 subunits (Bellone and Luscher, 2006; Luscher and Malenka, 2011). This GluR2-lacking receptor pool typically displays inward rectification (Isaac et al., 2007; Liu and Zukin, 2007), and one study confirms the appearance of this type of AMPAR following a single exposure to nicotine (Gao et al., 2010). Another study on nicotine (Baker et al., 2013) exposure to VTA DA neurons, however, demonstrated increases in AMPA/NMDA ratios but no appearance of an AMPAR pool displaying inward rectification. We find no appearance of inward rectification in AMPA-evoked currents (Fig. 4, B and D), which is more consistent with enhancement in numbers of GluR2-containing AMPARs rather than production of a significant amount of GluR2-lacking AMPARs. However, our data showing an increase in AMPAR sensitivity in response to α6β2* activation (Fig. 4F) supports a number of possible mechanisms, including increased AMPAR conductance

Downloaded from molpharm.aspetjournals.org at ASPET Journals on April 23, 2024

Molecular Pharmacology Fast Forward. Published on June 20, 2013 as DOI: 10.1124/mol.113.087346
This article has not been copyedited and formatted. The final version may differ from this version.

– a hallmark of GluR2-lacking AMPARs. Future pharmacological studies in α6L9′S and WT slices exposed to nicotine are needed to characterize AMPAR sensitivity changes.

What circuit and/or molecular signal transduction events following nicotine exposure are necessary and/or sufficient to enhance AMPAR function in VTA DA neurons? At the circuit level, an approach utilizing optogenetics demonstrated conclusively that in vivo activation of VTA DA neurons was sufficient to promote AMPAR redistribution (Brown et al., 2010). Because α6β2* nAChRs are selectively expressed in DA neurons in VTA (Drenan et al., 2008a; Mackey et al., 2012), our results lead us to favor a similar conclusion for nicotine: activation of α6β2* nAChRs on VTA DA neurons is sufficient to promote enhanced AMPAR function. Two other molecular events have been shown to be important for induction of synaptic plasticity in VTA DA neurons: D1/D5 DA receptor activation (Brown et al., 2010; Mao et al., 2011; Schilstrom et al., 2006), and NMDA receptor activation (Saal et al., 2003; Ungless et al., 2001). Although our SCH23390 results are inconclusive, NMDA receptor activation is necessary for α6β2* nAChR-mediated increases in AMPAR function (Fig. 6C). Together with previous studies on nicotine and other drugs of abuse, our data studying α6β2* nAChRs support the contention that there may be multiple mechanisms in place that nicotine can utilize to enhance the responsiveness of VTA DA neurons, ultimately leading to a heightened behavioral response to nicotine.

Conclusions and Future Studies

Our data show for the first time that activation of α4α6β2* nAChRs by nicotine is sufficient to stimulate a depolarizing conductance in VTA DA neurons as well as

Downloaded from molpharm.aspetjournals.org at ASPET Journals on April 23, 2024

Molecular Pharmacology Fast Forward. Published on June 20, 2013 as DOI: 10.1124/mol.113.087346
This article has not been copyedited and formatted. The final version may differ from this version.

enhance AMPAR function on the cell surface. Future studies should include determining the contribution of synaptic vs. extrasynaptic AMPARs, as well as studying whether acute exposure of intact animals to α6β2*-specific concentrations of nicotine is sufficient to drive changes in AMPAR function. Most importantly, it will be very important to report whether selective activation of α6β2* nAChRs is sufficient to support nicotine reward and/or reinforcement, and whether AMPAR activation plays a role in such behaviors. Such studies are ongoing. Together, our data show that α4α6β2* nAChRs are emerging as a key target for smoking cessation pharmacotherapy.

Downloaded from molpharm.aspetjournals.org at ASPET Journals on April 23, 2024

Molecular Pharmacology Fast Forward. Published on June 20, 2013 as DOI: 10.1124/mol.113.087346
This article has not been copyedited and formatted. The final version may differ from this version.

Acknowledgements

We thank members of the Drenan laboratory for helpful advice and discussions. Special thanks to Hilary Broderick, Gyeon Oh, and Karen Wethington for technical assistance.

Downloaded from molpharm.aspetjournals.org at ASPET Journals on April 23, 2024

Molecular Pharmacology Fast Forward. Published on June 20, 2013 as DOI: 10.1124/mol.113.087346
This article has not been copyedited and formatted. The final version may differ from this version.

Authorship Contributions

Participated in research design: Engle, Shih, and Drenan

Conducted experiments: Engle, Shih, and Drenan

Contributed new reagents or analytic tools: McIntosh

Performed data analysis: Engle, Shih, and Drenan

Wrote or contributed to the writing of the manuscript: Engle, McIntosh, and Drenan

Downloaded from molpharm.aspetjournals.org at ASPET Journals on April 23, 2024

Molecular Pharmacology Fast Forward. Published on June 20, 2013 as DOI: 10.1124/mol.113.087346
This article has not been copyedited and formatted. The final version may differ from this version.

References

Azam L, Maskos U, Changeux JP, Dowell CD, Christensen S, De Biasi M and McIntosh JM (2010) α-Conotoxin BuIA[T5A;P6O]: a novel ligand that discriminates between α6β4 and α6β2 nicotinic acetylcholine receptors and blocks nicotine-stimulated norepinephrine release. *FASEB J* **24**(12): 5113-5123.

Baker LK, Mao D, Chi H, Govind AP, Vallejo YF, Iacoviello M, Herrera S, Cortright JJ, Green WN, McGehee DS and Vezina P (2013) Intermittent nicotine exposure upregulates nAChRs in VTA dopamine neurons and sensitises locomotor responding to the drug. *Eur J Neurosci*.

Bellone C and Luscher C (2006) Cocaine triggered AMPA receptor redistribution is reversed in vivo by mGluR-dependent long-term depression. *Nat Neurosci* **9**(5): 636-641.

Brown MT, Bellone C, Mameli M, Labouebe G, Bocklisch C, Balland B, Dahan L, Lujan R, Deisseroth K and Luscher C (2010) Drug-driven AMPA receptor redistribution mimicked by selective dopamine neuron stimulation. *PLoS One* **5**(12): e15870.

Calabresi P, Lacey MG and North RA (1989) Nicotinic excitation of rat ventral tegmental neurones in vitro studied by intracellular recording. *Br J Pharmacol* **98**(1): 135-140.

Champtiaux N, Gotti C, Cordero-Erausquin M, David DJ, Przybylski C, Lena C, Clementi F, Moretti M, Rossi FM, Le Novere N, McIntosh JM, Gardier AM and Changeux JP (2003) Subunit composition of functional nicotinic receptors in dopaminergic neurons investigated with knock-out mice. *J Neurosci* **23**(21): 7820-7829.

Downloaded from molpharm.aspetjournals.org at ASPET Journals on April 23, 2024

Molecular Pharmacology Fast Forward. Published on June 20, 2013 as DOI: 10.1124/mol.113.087346
This article has not been copyedited and formatted. The final version may differ from this version.

Champtiaux N, Han ZY, Bessis A, Rossi FM, Zoli M, Marubio L, McIntosh JM and Changeux JP (2002) Distribution and pharmacology of α6-containing nicotinic acetylcholine receptors analyzed with mutant mice. *J Neurosci* **22**(4): 1208-1217.

Cohen BN, Mackey ED, Grady SR, McKinney S, Patzlaff NE, Wageman CR, McIntosh JM, Marks MJ, Lester HA and Drenan RM (2012) Nicotinic cholinergic mechanisms causing elevated dopamine release and abnormal locomotor behavior. *Neuroscience* **200**: 31-41.

Cui C, Booker TK, Allen RS, Grady SR, Whiteaker P, Marks MJ, Salminen O, Tritto T, Butt CM, Allen WR, Stitzel JA, McIntosh JM, Boulter J, Collins AC and Heinemann SF (2003) The β3 nicotinic receptor subunit: a component of α-Conotoxin MII-binding nicotinic acetylcholine receptors that modulate dopamine release and related behaviors. *J Neurosci* **23**(35): 11045-11053.

Di Chiara G and Imperato A (1988) Drugs abused by humans preferentially increase synaptic dopamine concentrations in the mesolimbic system of freely moving rats. *Proc Natl Acad Sci U S A* **85**(14): 5274-5278.

Drenan RM, Grady SR, Steele AD, McKinney S, Patzlaff NE, McIntosh JM, Marks MJ, Miwa JM and Lester HA (2010) Cholinergic modulation of locomotion and striatal dopamine release is mediated by α6α4* nicotinic acetylcholine receptors. *J Neurosci* **30**(29): 9877-9889.

Drenan RM, Grady SR, Whiteaker P, McClure-Begley T, McKinney S, Miwa JM, Bupp S, Heintz N, McIntosh JM, Bencherif M, Marks MJ and Lester HA (2008a) *In vivo* activation of midbrain dopamine neurons via sensitized, high-affinity α6* nicotinic acetylcholine receptors. *Neuron* **60**(1): 123-136.

Downloaded from molpharm.aspetjournals.org at ASPET Journals on April 23, 2024

Molecular Pharmacology Fast Forward. Published on June 20, 2013 as DOI: 10.1124/mol.113.087346
This article has not been copyedited and formatted. The final version may differ from this version.

Drenan RM and Lester HA (2012) Insights into the Neurobiology of the Nicotinic Cholinergic System and Nicotine Addiction from Mice Expressing Nicotinic Receptors Harboring Gain-of-Function Mutations. *Pharmacol Rev*.

Drenan RM, Nashmi R, Imoukhuede P, Just H, McKinney S and Lester HA (2008b) Subcellular trafficking, pentameric assembly, and subunit stoichiometry of neuronal nicotinic acetylcholine receptors containing fluorescently labeled α6 and β3 subunits. *Mol Pharmacol* **73**(1): 27-41.

Engle SE, Broderick HJ and Drenan RM (2012) Local application of drugs to study nicotinic acetylcholine receptor function in mouse brain slices. *J Vis Exp*(68): e50034.

Fowler CD, Lu Q, Johnson PM, Marks MJ and Kenny PJ (2011) Habenular α5 nicotinic receptor subunit signalling controls nicotine intake. *Nature* **471**(7340): 597-601.

Gao C and Wolf ME (2007) Dopamine alters AMPA receptor synaptic expression and subunit composition in dopamine neurons of the ventral tegmental area cultured with prefrontal cortex neurons. *J Neurosci* **27**(52): 14275-14285.

Gao M, Jin Y, Yang K, Zhang D, Lukas RJ and Wu J (2010) Mechanisms involved in systemic nicotine-induced glutamatergic synaptic plasticity on dopamine neurons in the ventral tegmental area. *J Neurosci* **30**(41): 13814-13825.

Gotti C, Guiducci S, Tedesco V, Corbioli S, Zanetti L, Moretti M, Zanardi A, Rimondini R, Mugnaini M, Clementi F, Chiamulera C and Zoli M (2010) Nicotinic acetylcholine receptors in the mesolimbic pathway: primary role of ventral tegmental area α6β2* receptors in mediating systemic nicotine effects on

Downloaded from molpharm.aspetjournals.org at ASPET Journals on April 23, 2024

Molecular Pharmacology Fast Forward. Published on June 20, 2013 as DOI: 10.1124/mol.113.087346
This article has not been copyedited and formatted. The final version may differ from this version.

dopamine release, locomotion, and reinforcement. *J Neurosci* **30**(15): 5311-5325.

Grady SR, Murphy KL, Cao J, Marks MJ, McIntosh JM and Collins AC (2002) Characterization of nicotinic agonist-induced [^{3}H]dopamine release from synaptosomes prepared from four mouse brain regions. *J Pharmacol Exp Ther* **301**(2): 651-660.

Isaac JT, Ashby MC and McBain CJ (2007) The role of the GluR2 subunit in AMPA receptor function and synaptic plasticity. *Neuron* **54**(6): 859-871.

Itier V and Bertrand D (2001) Neuronal nicotinic receptors: from protein structure to function. *FEBS Lett* **504**(3): 118-125.

Jin Y, Yang K, Wang H and Wu J (2011) Exposure of nicotine to ventral tegmental area slices induces glutamatergic synaptic plasticity on dopamine neurons. *Synapse* **65**(4): 332-338.

Kauer JA and Malenka RC (2007) Synaptic plasticity and addiction. *Nat Rev Neurosci* **8**(11): 844-858.

Kobayashi M, Kojima M, Koyanagi Y, Adachi K, Imamura K and Koshikawa N (2009) Presynaptic and postsynaptic modulation of glutamatergic synaptic transmission by activation of α1- and β-adrenoceptors in layer V pyramidal neurons of rat cerebral cortex. *Synapse* **63**(4): 269-281.

Kuryatov A and Lindstrom J (2011) Expression of functional human $\alpha6\beta2\beta3$* acetylcholine receptors in *Xenopus laevis* oocytes achieved through subunit chimeras and concatamers. *Mol Pharmacol* **79**(1): 126-140.

Downloaded from molpharm.aspetjournals.org at ASPET Journals on April 23, 2024

Molecular Pharmacology Fast Forward. Published on June 20, 2013 as DOI: 10.1124/mol.113.087346
This article has not been copyedited and formatted. The final version may differ from this version.

Labarca C, Nowak MW, Zhang H, Tang L, Deshpande P and Lester HA (1995) Channel gating governed symmetrically by conserved leucine residues in the M2 domain of nicotinic receptors. *Nature* **376**(6540): 514-516.

Lammel S, Hetzel A, Hackel O, Jones I, Liss B and Roeper J (2008) Unique properties of mesoprefrontal neurons within a dual mesocorticolimbic dopamine system. *Neuron* **57**(5): 760-773.

Lammel S, Ion DI, Roeper J and Malenka RC (2011) Projection-specific modulation of dopamine neuron synapses by aversive and rewarding stimuli. *Neuron* **70**(5): 855-862.

Laviolette SR and van der Kooy D (2004) The neurobiology of nicotine addiction: bridging the gap from molecules to behaviour. *Nat Rev Neurosci* **5**(1): 55-65.

Le Novere N, Zoli M and Changeux JP (1996) Neuronal nicotinic receptor α6 subunit mRNA is selectively concentrated in catecholaminergic nuclei of the rat brain. *Eur J Neurosci* **8**(11): 2428-2439.

Lena C, de Kerchove D'Exaerde A, Cordero-Erausquin M, Le Novere N, del Mar Arroyo-Jimenez M and Changeux JP (1999) Diversity and distribution of nicotinic acetylcholine receptors in the locus ceruleus neurons. *Proc Natl Acad Sci U S A* **96**(21): 12126-12131.

Li DP, Yang Q, Pan HM and Pan HL (2008) Pre- and postsynaptic plasticity underlying augmented glutamatergic inputs to hypothalamic presympathetic neurons in spontaneously hypertensive rats. *J Physiol* **586**(6): 1637-1647.

Downloaded from molpharm.aspetjournals.org at ASPET Journals on April 23, 2024

Molecular Pharmacology Fast Forward. Published on June 20, 2013 as DOI: 10.1124/mol.113.087346
This article has not been copyedited and formatted. The final version may differ from this version.

Liu L, Zhao-Shea R, McIntosh JM, Gardner P and Tapper A (2012) Nicotine Persistently Activates Ventral Tegmental Area Dopaminergic Neurons Via Nicotinic Acetylcholine Receptors Containing α4 and α6 subunits. *Mol Pharmacol*.

Liu SJ and Zukin RS (2007) Ca^{2+}-permeable AMPA receptors in synaptic plasticity and neuronal death. *Trends Neurosci* **30**(3): 126-134.

Luscher C and Malenka RC (2011) Drug-evoked synaptic plasticity in addiction: from molecular changes to circuit remodeling. *Neuron* **69**(4): 650-663.

Mackey ED, Engle SE, Kim MR, O'Neill HC, Wageman CR, Patzlaff NE, Wang Y, Grady SR, McIntosh JM, Marks MJ, Lester HA and Drenan RM (2012) α6* Nicotinic Acetylcholine Receptor Expression and Function in a Visual Salience Circuit. *J Neurosci* **32**(30): 10226-10237.

Mansvelder HD, Keath JR and McGehee DS (2002) Synaptic mechanisms underlie nicotine-induced excitability of brain reward areas. *Neuron* **33**(6): 905-919.

Mansvelder HD and McGehee DS (2000) Long-term potentiation of excitatory inputs to brain reward areas by nicotine. *Neuron* **27**(2): 349-357.

Mao D, Gallagher K and McGehee DS (2011) Nicotine potentiation of excitatory inputs to ventral tegmental area dopamine neurons. *J Neurosci* **31**(18): 6710-6720.

Maskos U, Molles BE, Pons S, Besson M, Guiard BP, Guilloux JP, Evrard A, Cazala P, Cormier A, Mameli-Engvall M, Dufour N, Cloez-Tayarani I, Bemelmans AP, Mallet J, Gardier AM, David V, Faure P, Granon S and Changeux JP (2005) Nicotine reinforcement and cognition restored by targeted expression of nicotinic receptors. *Nature* **436**(7047): 103-107.

Downloaded from molpharm.aspetjournals.org at ASPET Journals on April 23, 2024

Molecular Pharmacology Fast Forward. Published on June 20, 2013 as DOI: 10.1124/mol.113.087346
This article has not been copyedited and formatted. The final version may differ from this version.

Nashmi R, Xiao C, Deshpande P, McKinney S, Grady SR, Whiteaker P, Huang Q, McClure-Begley T, Lindstrom JM, Labarca C, Collins AC, Marks MJ and Lester HA (2007) Chronic nicotine cell specifically upregulates functional α4* nicotinic receptors: basis for both tolerance in midbrain and enhanced long-term potentiation in perforant path. *J Neurosci* **27**(31): 8202-8218.

Peto R and Lopez AD (2001) Future worldwide health effects of current smoking patterns, in *Critical Issues in Global Health* (Koop CE, Pearson CE and Schwarz MR eds) pp 154-161, Jossey-Bass, San Francisco.

Picciotto MR, Addy NA, Mineur YS and Brunzell DH (2008) It is not "either/or": activation and desensitization of nicotinic acetylcholine receptors both contribute to behaviors related to nicotine addiction and mood. *Prog Neurobiol* **84**(4): 329-342.

Picciotto MR, Zoli M, Rimondini R, Lena C, Marubio LM, Pich EM, Fuxe K and Changeux JP (1998) Acetylcholine receptors containing the β2 subunit are involved in the reinforcing properties of nicotine. *Nature* **391**(6663): 173-177.

Pidoplichko VI, DeBiasi M, Williams JT and Dani JA (1997) Nicotine activates and desensitizes midbrain dopamine neurons. *Nature* **390**(6658): 401-404.

Pons S, Fattore L, Cossu G, Tolu S, Porcu E, McIntosh JM, Changeux JP, Maskos U and Fratta W (2008) Crucial role of α4 and α6 nicotinic acetylcholine receptor subunits from ventral tegmental area in systemic nicotine self-administration. *J Neurosci* **28**(47): 12318-12327.

Downloaded from molpharm.aspetjournals.org at ASPET Journals on April 23, 2024

Molecular Pharmacology Fast Forward. Published on June 20, 2013 as DOI: 10.1124/mol.113.087346
This article has not been copyedited and formatted. The final version may differ from this version.

Revah F, Bertrand D, Galzi JL, Devillers-Thiery A, Mulle C, Hussy N, Bertrand S, Ballivet M and Changeux JP (1991) Mutations in the channel domain alter desensitization of a neuronal nicotinic receptor. *Nature* **353**(6347): 846-849.

Saal D, Dong Y, Bonci A and Malenka RC (2003) Drugs of abuse and stress trigger a common synaptic adaptation in dopamine neurons. *Neuron* **37**(4): 577-582.

Salminen O, Drapeau JA, McIntosh JM, Collins AC, Marks MJ and Grady SR (2007) Pharmacology of α-Conotoxin MII-Sensitive Subtypes of Nicotinic Acetylcholine Receptors Isolated by Breeding of Null Mutant Mice. *Mol Pharmacol* **71**(6): 1563-1571.

Salminen O, Murphy KL, McIntosh JM, Drago J, Marks MJ, Collins AC and Grady SR (2004) Subunit composition and pharmacology of two classes of striatal presynaptic nicotinic acetylcholine receptors mediating dopamine release in mice. *Mol Pharmacol* **65**(6): 1526-1535.

Sanchez JT, Wang Y, Rubel EW and Barria A (2010) Development of glutamatergic synaptic transmission in binaural auditory neurons. *J Neurophysiol* **104**(3): 1774-1789.

Schilstrom B, Yaka R, Argilli E, Suvarna N, Schumann J, Chen BT, Carman M, Singh V, Mailliard WS, Ron D and Bonci A (2006) Cocaine enhances NMDA receptor-mediated currents in ventral tegmental area cells via dopamine D5 receptor-dependent redistribution of NMDA receptors. *J Neurosci* **26**(33): 8549-8558.

Tapper AR, McKinney SL, Nashmi R, Schwarz J, Deshpande P, Labarca C, Whiteaker P, Marks MJ, Collins AC and Lester HA (2004) Nicotine activation of α4*

Downloaded from molpharm.aspetjournals.org at ASPET Journals on April 23, 2024

Molecular Pharmacology Fast Forward. Published on June 20, 2013 as DOI: 10.1124/mol.113.087346
This article has not been copyedited and formatted. The final version may differ from this version.

receptors: sufficient for reward, tolerance, and sensitization. *Science* **306**(5698): 1029-1032.

Ungless MA, Whistler JL, Malenka RC and Bonci A (2001) Single cocaine exposure in vivo induces long-term potentiation in dopamine neurons. *Nature* **411**(6837): 583-587.

Wolf ME, Sun X, Mangiavacchi S and Chao SZ (2004) Psychomotor stimulants and neuronal plasticity. *Neuropharmacology* **47 Suppl 1**: 61-79.

Wooltorton JR, Pidoplichko VI, Broide RS and Dani JA (2003) Differential desensitization and distribution of nicotinic acetylcholine receptor subtypes in midbrain dopamine areas. *J Neurosci* **23**(8): 3176-3185.

Yang K, Buhlman L, Khan GM, Nichols RA, Jin G, McIntosh JM, Whiteaker P, Lukas RJ and Wu J (2011) Functional Nicotinic Acetylcholine Receptors Containing α6 Subunits Are on GABAergic Neuronal Boutons Adherent to Ventral Tegmental Area Dopamine Neurons. *J Neurosci* **31**(7): 2537-2548.

Zhang TA, Placzek AN and Dani JA (2010) In vitro identification and electrophysiological characterization of dopamine neurons in the ventral tegmental area. *Neuropharmacology* **59**(6): 431-436.

Zhao-Shea R, Liu L, Soll LG, Improgo MR, Meyers EE, McIntosh JM, Grady SR, Marks MJ, Gardner PD and Tapper AR (2011) Nicotine-mediated activation of dopaminergic neurons in distinct regions of the ventral tegmental area. *Neuropsychopharmacology* **36**(5): 1021-1032.

Downloaded from molpharm.aspetjournals.org at ASPET Journals on April 23, 2024

Molecular Pharmacology Fast Forward. Published on June 20, 2013 as DOI: 10.1124/mol.113.087346
This article has not been copyedited and formatted. The final version may differ from this version.

Footnotes

This work was supported by the National Institutes of Health National Institute on Drug Abuse [DA030396], National Institute of General Medical Sciences [GM48677], [GM103801] and the Ralph W. and Grace M. Showalter Research Trust.

S. Engle was supported by a Purdue University Frederick N. Andrews Fellowship.

Reprint requests should be directed to Ryan M. Drenan (575 Stadium Mall Dr., West Lafayette, IN 47907; drenan@purdue.edu).

Downloaded from molpharm.aspetjournals.org at ASPET Journals on April 23, 2024

Molecular Pharmacology Fast Forward. Published on June 20, 2013 as DOI: 10.1124/mol.113.087346
This article has not been copyedited and formatted. The final version may differ from this version.

Figure Legends

Figure 1. Electrophysiological identification of VTA DA neurons. **A:** Whole-cell current-clamp recordings of VTA DA neurons show spontaneous (I = 0 pA), pacemaker firing (1-5 Hz) and "sag" responses in the membrane potential in response to hyperpolarizing (I = -120 pA) current injections. **B:** VTA DA neurons have wide action potentials. The neuron in **A** indicated with an arrow is shown on an expanded time scale to better view the action potential width (typically 2-5 msec) seen in the neurons under study. **C:** I_h currents in VTA DA neurons. VTA cells were held at -60 mV in voltage-clamp mode and membrane current was recorded at baseline and during a voltage step to -120 mV.

D: Single cell RT-PCR. VTA neurons recorded in whole cell mode were aspirated into the recording pipette, followed by reverse-transcription of RNA and subsequent PCR reactions to detect TH and GAPDH (positive control) expression. Expected band sizes are as follows: TH = 207 bp, GAPDH = 138 bp (* indicates a spurious PCR reaction, possibly generated from external primer pairs). As a negative control, a pipette was lowered into the slice and mild negative pressure was applied. The pipette was removed from the slice and assayed with RT-PCR as for a recorded cell.

Figure 2. A low concentration of nicotine is sufficient to increase inward currents in VTA DA neurons.

A: α6L9′S or non-Tg control neurons were voltage clamped in whole-cell mode. Inhibitor cocktail (10 μM CNQX, 75 μM picrotoxin, 0.5 μM TTX) was superfused, followed by nicotine (100 nM), then αCtxMII (100 nM). A representative experiment

Downloaded from molpharm.aspetjournals.org at ASPET Journals on April 23, 2024

Molecular Pharmacology Fast Forward. Published on June 20, 2013 as DOI: 10.1124/mol.113.087346
This article has not been copyedited and formatted. The final version may differ from this version.

from a α6L9′S neuron is shown. Expanded recordings from time points (i), (ii), and (iii) are shown in B-D below,

B-D: Voltage clamp recording segments from α6L9′S (B; 100 nM nicotine), non-Tg (C; 100 nM nicotine), and non-Tg (D; 300 nM nicotine) VTA DA neurons at 1) baseline with inhibitor cocktail present (i), 2) inhibitor cocktail plus nicotine (ii), and 3) inhibitor cocktail/nicotine plus αCtxMII (iii).

E: Summary showing mean holding current (-pA) change from baseline in response to nicotine, and nicotine plus αCtxMII in the indicated mouse strain (α6L9′S and non-Tg littermate). *p<0.05

Figure 3. AMPA-evoked current methodology. **A.** A drug-filled pipette is positioned above/next to the cell being recorded. A piezoelectric translator brings the pipette close (20 - 40 µm) to the cell, a TTL pulse triggers a pressure ejection that dispenses drug (AMPA) onto the cell, and the piezoelectric translator withdraws the pipette away from the cell. **B:** Representative recording showing the timing of the TTL pulse, piezo drive movement, and resulting inward current elicited by application of 100 µM AMPA to a VTA DA neuron.

Figure 4. Activation of α6* nAChRs is sufficient to enhance AMPAR function on the surface of VTA DA neurons.

A: Slice treatment procedure. Brain slices from adult α6L9′S and non-Tg littermate mice were cut, recovered for 60 min, and incubated for 60 min in control recording

Downloaded from molpharm.aspetjournals.org at ASPET Journals on April 23, 2024

Molecular Pharmacology Fast Forward. Published on June 20, 2013 as DOI: 10.1124/mol.113.087346
This article has not been copyedited and formatted. The final version may differ from this version.

solution or recording solution plus nicotine (100 nM). Nicotine was washed out for ≥ 60 min, and whole-cell recordings were established in VTA DA neurons.

B. AMPA currents were evoked by puff-application of AMPA (100 μM) at holding potentials of -60 mV, 0 mV, and +40 mV. Representative recordings from incubation of slices in control and nicotine solutions are shown for α6L9′S and non-Tg littermate mice.

C & D: Summary showing mean AMPA-evoked currents ([AMPA] = 100 μM) in non-Tg littermate (**B**) and α6L9′S (**C**) VTA DA neurons in response to control incubation or nicotine incubation at the indicated concentration. Number of observations were as follows: non-Tg control (-60 mV = 10, 0 mV = 7, +40 mV = 7); non-Tg 100 nM nicotine (-60 mV = 4, 0 mV = 4, +40 mV = 4); non-Tg 500 nM nicotine (-60 mV = 16, 0 mV = 12, +40 mV = 12); α6L9′S control (-60 mV = 14, 0 mV = 13, +40 mV = 13); α6L9′S 100 nM nicotine (-60 mV = 11, 0 mV = 11, +40 mV = 11).

E: AMPA concentration-response curve in VTA DA neurons. AMPA-evoked currents were measured in non-Tg and α6L9′S neurons. AMPA concentrations and number of observations at each data point are as follows: non-Tg (1 μM, n = 2; 10 μM, n = 6; 50 μM, n = 5; 100 μM, n = 10; 250 μM, n = 5; 500 μM, n = 14; 1000 μM, n = 11), α6L9′S (1 μM, n = 2; 10 μM, n = 4; 50 μM, n = 4; 100 μM, n = 14; 250 μM, n = 5; 500 μM, n = 4; 1000 μM, n = 5; 3000 μM, n = 2). Data (mean ± SEM) were fitted to the Hill equation, and EC_{50} (± 95% confidence interval) for each curve is plotted.

F: AMPA concentration-response curve in α6L9′S VTA DA neurons. AMPA-evoked currents were measured in α6L9′S control slices or slices incubated in 100 nM nicotine for 60 min followed by > 60 min washout prior to recording. Control treated α6L9′S data from **E** are re-plotted here for reference. AMPA concentrations and number of

Downloaded from molpharm.aspetjournals.org at ASPET Journals on April 23, 2024

Molecular Pharmacology Fast Forward. Published on June 20, 2013 as DOI: 10.1124/mol.113.087346
This article has not been copyedited and formatted. The final version may differ from this version.

observations at each data point for α6L9′S slices treated with nicotine are as follows: α6L9′S (1 μM, n = 2; 10 μM, n = 3; 50 μM, n = 2; 100 μM, n = 11; 300 μM, n = 3; 1000 μM, n = 3). Data (mean ± SEM) were fitted to the Hill equation and EC_{50} (± 95% confidence interval) for each curve is plotted.

Figure 5. Time-dependence for enhancement of AMPA-evoked currents in α6L9′S VTA DA neurons.

A: Slice treatment procedure. Brain slices from α6L9′S mice were cut and recovered for 60 min. Slices were then incubated in nicotine (100 nM) for either 10 or 60 min, followed in either case by a washout period of ≥ 60 min. Some slices treated with nicotine for 60 min were allowed > 240 min of washout prior to recording.

B: Representative AMPA-evoked currents ([AMPA] = 100 μM) at +40 mV and -60 mV in VTA DA neurons in response to treatment detailed in **A**.

C: Summary showing mean (± SEM) AMPA-evoked ([AMPA] = 100 μM) current in α6L9′S VTA DA neurons in response to the conditions described in **A**.

Figure 6. Pharmacology of AMPA-evoked current induction in α6L9′S VTA DA neurons.

A: Slice treatment procedure. α6L9′S brain slices were cut and recovered for 60 min. Slices were pre-treated for 10 min with one of the drugs indicated in **B**, followed by co-treatment with the drug plus nicotine (100 nM) for 60 min. Slices were washed out for > 60 min prior to recording.

B: Representative AMPA-evoked currents ([AMPA] = 100 μM) at +40 mV and -60 mV in VTA DA neurons from α6L9′S brain slices pre-exposed for 10 min to either control recording solution or the following drugs followed by incubation in 100 nM nicotine for

Downloaded from molpharm.aspetjournals.org at ASPET Journals on April 23, 2024

Molecular Pharmacology Fast Forward. Published on June 20, 2013 as DOI: 10.1124/mol.113.087346
This article has not been copyedited and formatted. The final version may differ from this version.

60 min: (MII = α-conotoxin MII; SCH = SCH23390; AP5 = (2*R*)-amino-5-phosphonovaleric acid; MLA = methyllycaconitine A).

C: Summary showing mean (± SEM) AMPA-evoked currents ([AMPA] = 100 μM) in α6L9′S VTA DA neurons in response to the conditions described in **A**.

Figure 7. Enhanced AMPA-evoked currents in α6L9′S VTA DA neurons are mediated, in part, by α4 nAChR subunits.

A: Slice treatment procedure. Brain slices from adult α6L9′S and α6L9′Sα4KO littermate mice were cut, recovered for 60 min, and incubated for 60 min in control recording solution or recording solution plus nicotine (100 nM). Nicotine was washed out for ≥ 60 min, and whole-cell recordings were established in VTA DA neurons.

B: Representative AMPA-evoked currents ([AMPA] = 100 μM) at +40 mV and -60 mV in VTA DA neurons from α6L9′S and α6L9′Sα4KO brain slices following incubation in 100 nM nicotine for 60 min.

C: Summary showing mean (± SEM) AMPA-evoked currents ([AMPA] = 100 μM) in α6L9′S and α6L9′Sα4KO VTA DA neurons in response to the conditions described in **A**.

Figure 8. α6* nAChR function is reduced in α4KO mice.

A: Schematic of α6GFP transgenic mice and α6GFP nAChRs.

B: The resulting α6* nAChR that remains following crossing α6GFP mice to α4KO mice is shown.

C: α6* nAChRs were quantified in α6GFP and α6GFPα4KO VTA DA neurons using anti-GFP immunohistochemistry and confocal microscopy. Mean per-cell pixel intensity for each genotype is shown.

Downloaded from molpharm.aspetjournals.org at ASPET Journals on April 23, 2024

Molecular Pharmacology Fast Forward. Published on June 20, 2013 as DOI: 10.1124/mol.113.087346
This article has not been copyedited and formatted. The final version may differ from this version.

D: The resulting α6* nAChR that remains following crossing α6L9′S mice to α4KO mice is shown.

E: Representative ACh-evoked currents in α6L9′S and α6L9′Sα4KO VTA DA neurons. VTA DA neurons from both genotypes were patch-clamped and ACh was puff-applied (250 msec) at the indicated concentration.

F: Summary showing mean (± SEM) ACh-evoked current in α6L9′S and α6L9′Sα4KO VTA DA neurons in response to the indicated concentration of ACh.

G: Representative nicotine-evoked currents in α6L9′S and α6L9′Sα4KO VTA DA neurons. VTA DA neurons from both genotypes were patch-clamped and nicotine was puff-applied at the indicated concentration.

H: Summary showing mean (± SEM) nicotine-evoked current in α6L9′S and α6L9′Sα4KO VTA DA neurons in response to the indicated concentration of nicotine.

Figure 9. NMDA-evoked currents are not changed by nicotine in α6L9′S VTA DA neurons.

A: Slice treatment procedure. Brain slices from adult α6L9′S and non-Tg littermate mice were cut, recovered for 60 min, and incubated for 60 min in control recording solution or recording solution plus nicotine (100 nM). Nicotine was washed out for ≥ 60 min, and whole-cell recordings were established in VTA DA neurons.

B: Representative NMDA-evoked currents ([NMDA] = 100 μM) at +40 mV in VTA DA neurons from α6L9′S and non-Tg littermate brain slices in response to control incubation or incubation in 100 nM nicotine for 60 min.

Downloaded from molpharm.aspetjournals.org at ASPET Journals on April 23, 2024

Molecular Pharmacology Fast Forward. Published on June 20, 2013 as DOI: 10.1124/mol.113.087346
This article has not been copyedited and formatted. The final version may differ from this version.

C: Summary showing mean (± SEM) NMDA-evoked currents ([NMDA] = 100 μM) in α6L9′S and non-Tg littermate VTA DA neurons in response to the conditions described in **A**.

Downloaded from molpharm.aspetjournals.org at ASPET Journals on April 23, 2024

Figure 1

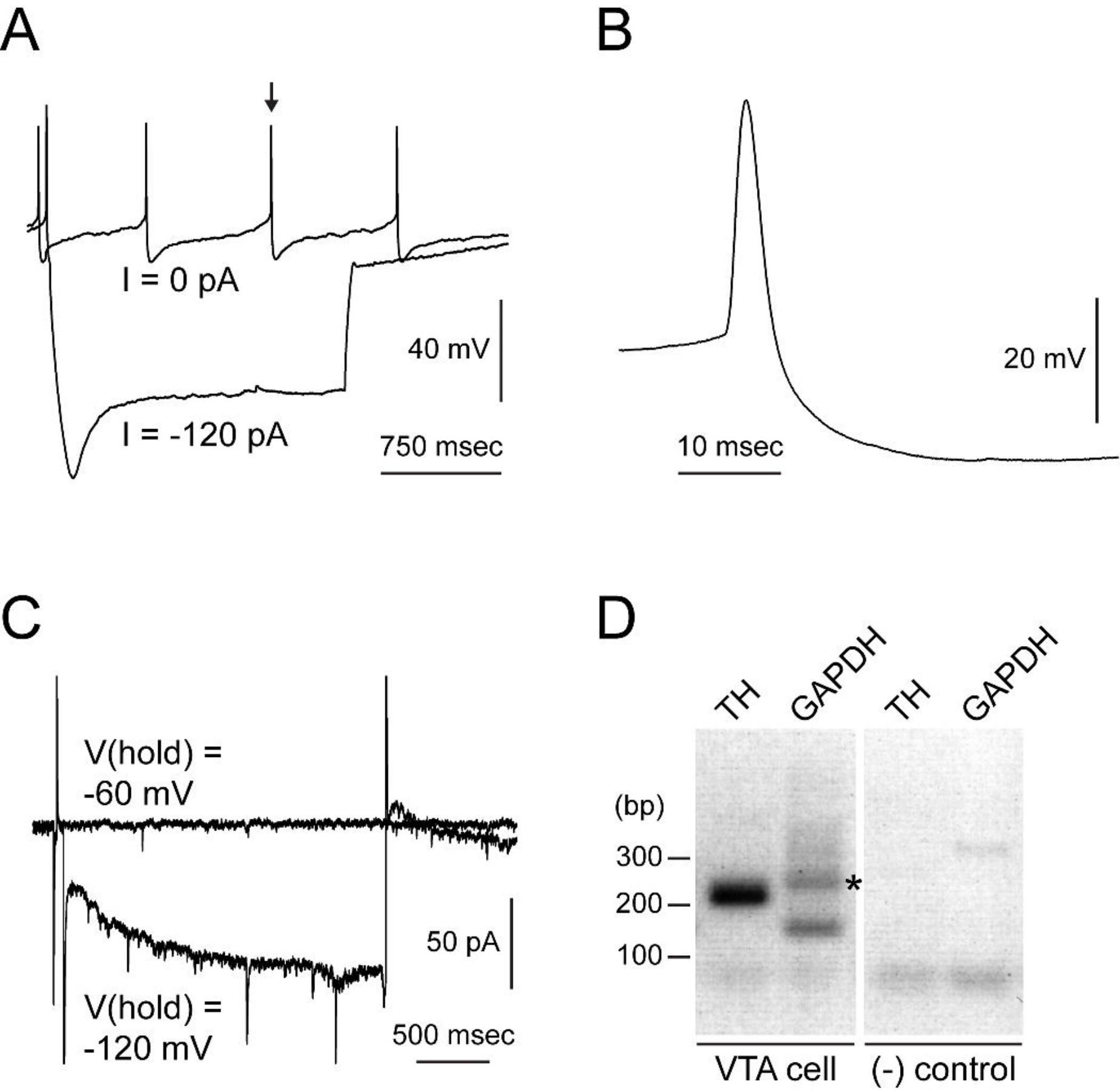
A
I = 0 pA
40 mV
I = -120 pA
750 msec
B
20 mV
10 msec
C
V(hold) =
-60 mV
50 pA
V(hold) =
-120 mV
500 msec
D
TH
GAPDH
TH
GAPDH
(bp)
300
200
100
*
VTA cell
(-) control

Figure 2

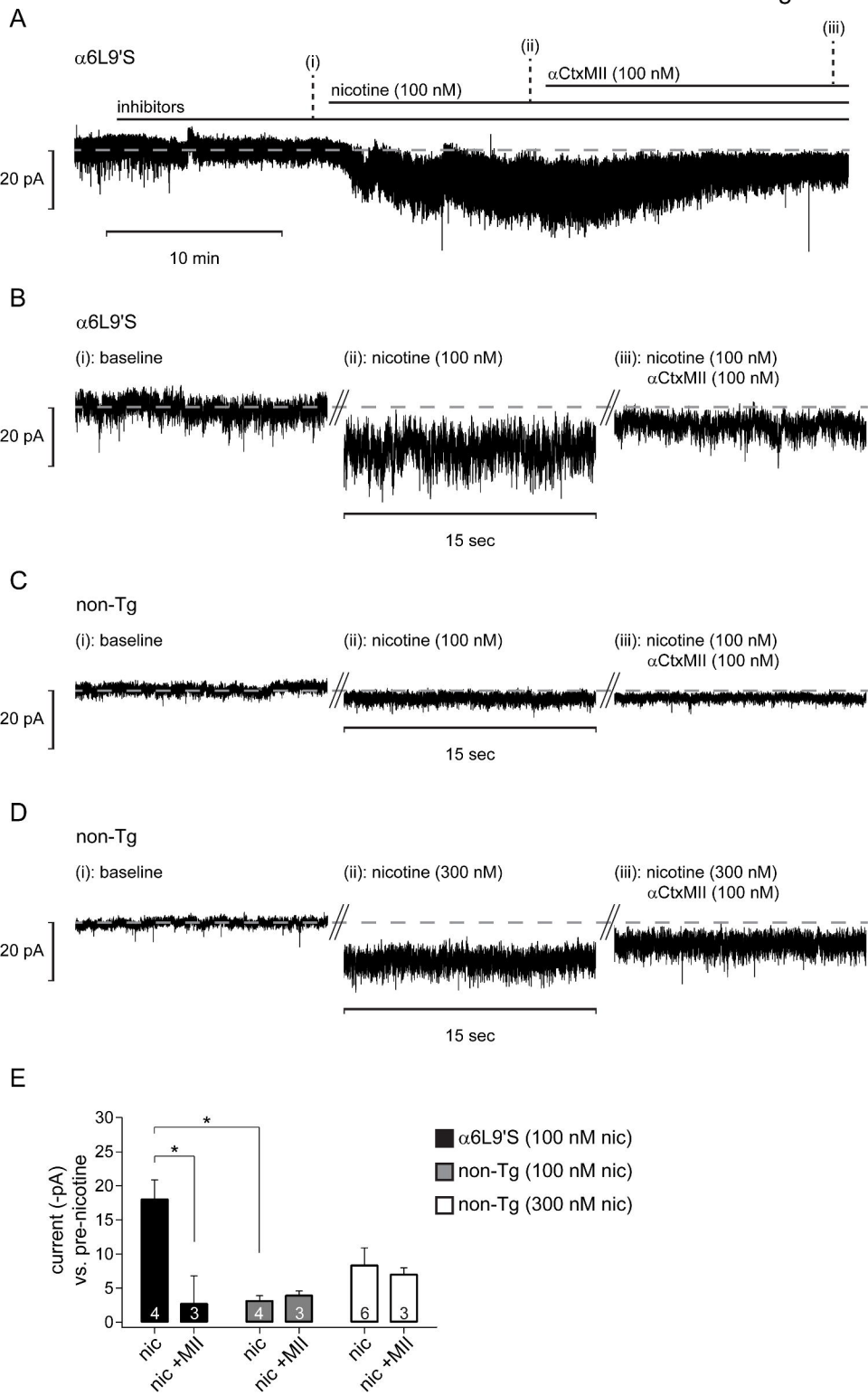
A
α6L9'S
(i)
(ii)
(iii)
nicotine (100 nM)
αCtxMII (100 nM)
inhibitors
20 pA
10 min
B
α6L9'S
(i): baseline
(ii): nicotine (100 nM)
(iii): nicotine (100 nM)
αCtxMII (100 nM)
20 pA
15 sec
C
non-Tg
(i): baseline
(ii): nicotine (100 nM)
(iii): nicotine (100 nM)
αCtxMII (100 nM)
20 pA
15 sec
D
non-Tg
(i): baseline
(ii): nicotine (300 nM)
(iii): nicotine (300 nM)
αCtxMII (100 nM)
20 pA
15 sec
E
current (-pA)
vs. pre-nicotine
30
25
20
15
10
5
0
*
*
4
3
4
3
6
3
nic
nic +MII
nic
nic +MII
nic
nic +MII
α6L9'S (100 nM nic)
non-Tg (100 nM nic)
non-Tg (300 nM nic)

Figure 3

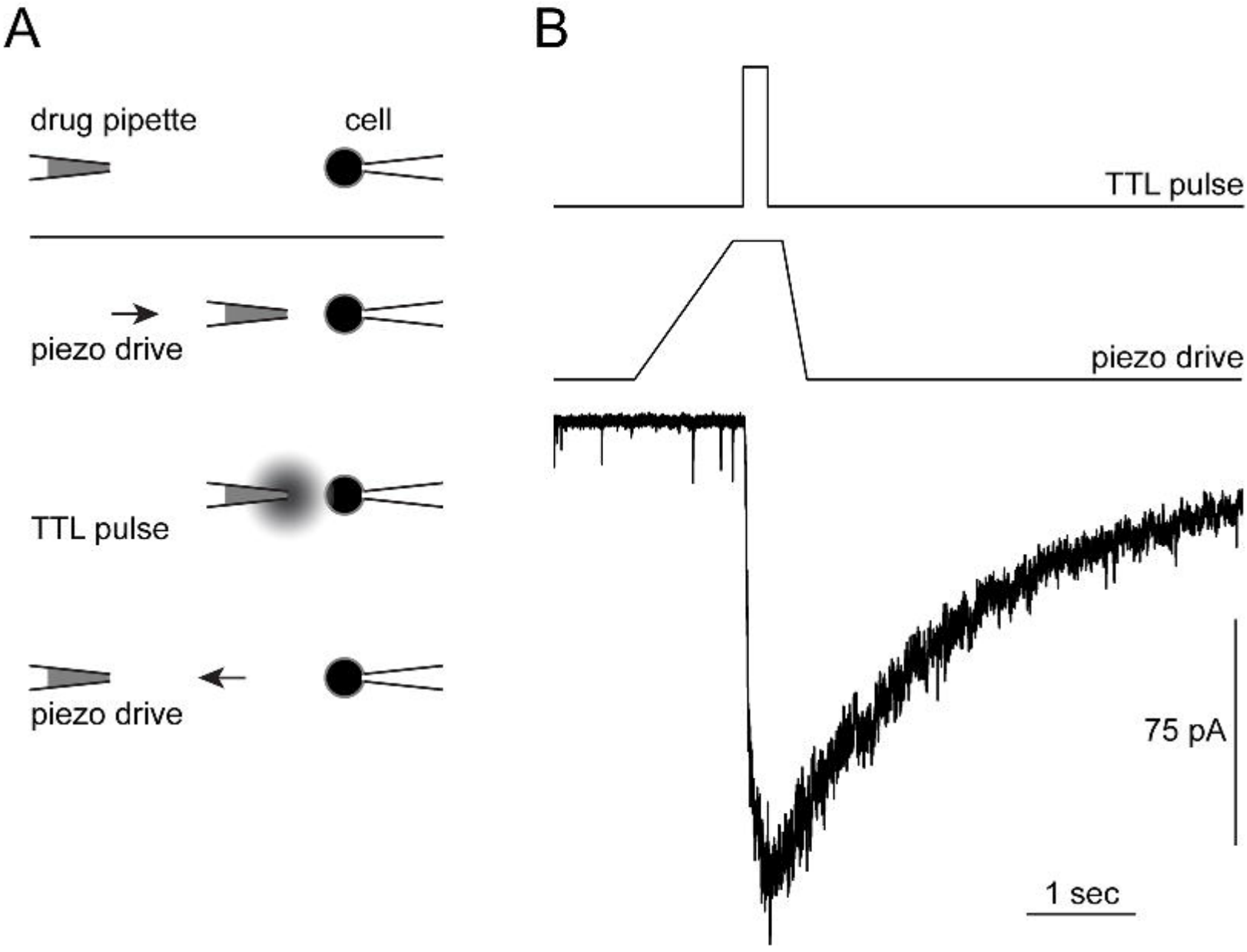
A
drug pipette
cell
piezo drive
TTL pulse
piezo drive
B
TTL pulse
piezo drive
75 pA
1 sec

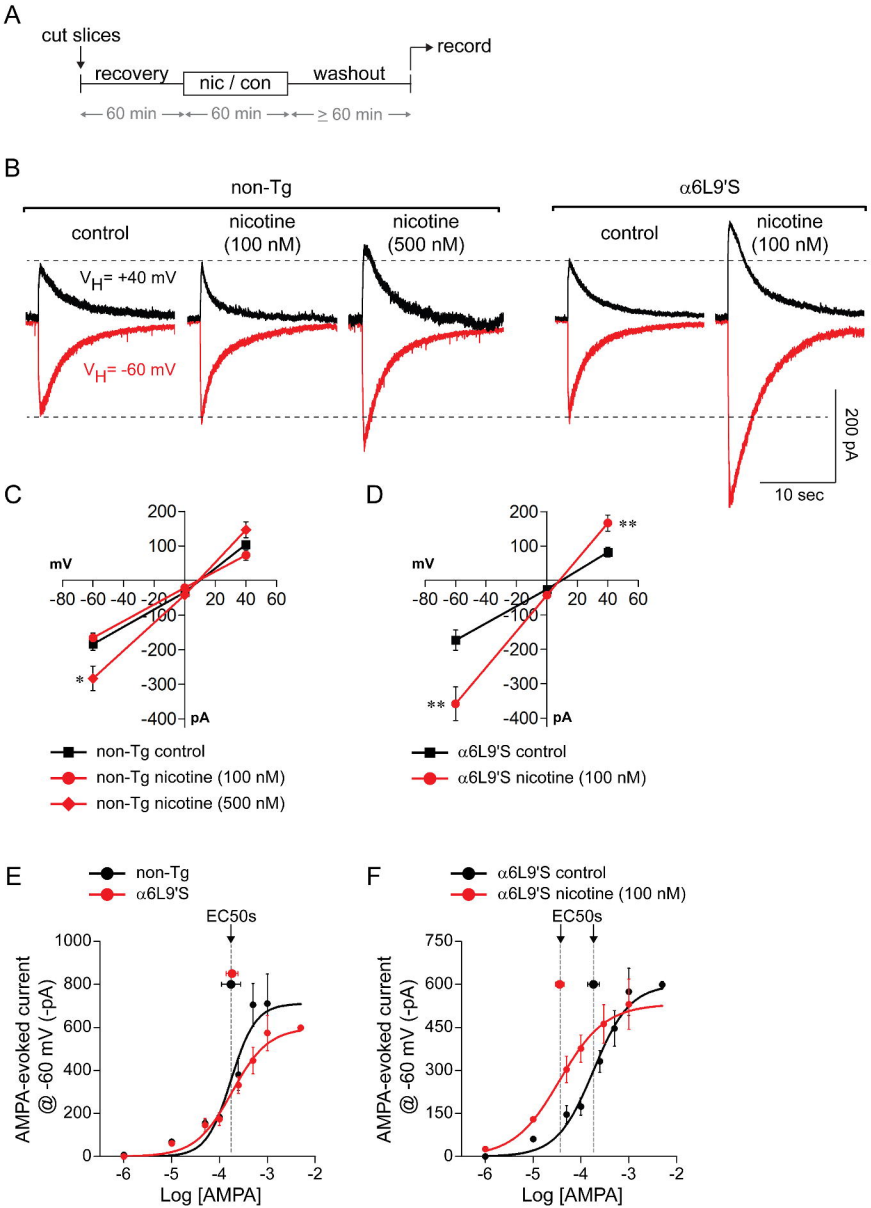
A
cut slices
recovery
nic / con
washout
record
60 min
60 min
≥ 60 min
B
non-Tg
α6L9'S
control
nicotine (100 nM)
nicotine (500 nM)
control
nicotine (100 nM)
V_H= +40 mV
V_H= -60 mV
200 pA
10 sec
C
mV
pA
non-Tg control
non-Tg nicotine (100 nM)
non-Tg nicotine (500 nM)
D
mV
pA
α6L9'S control
α6L9'S nicotine (100 nM)
E
non-Tg
α6L9'S
EC50s
AMPA-evoked current @ -60 mV (-pA)
Log [AMPA]
F
α6L9'S control
α6L9'S nicotine (100 nM)
EC50s
AMPA-evoked current @ -60 mV (-pA)
Log [AMPA]

Figure 5

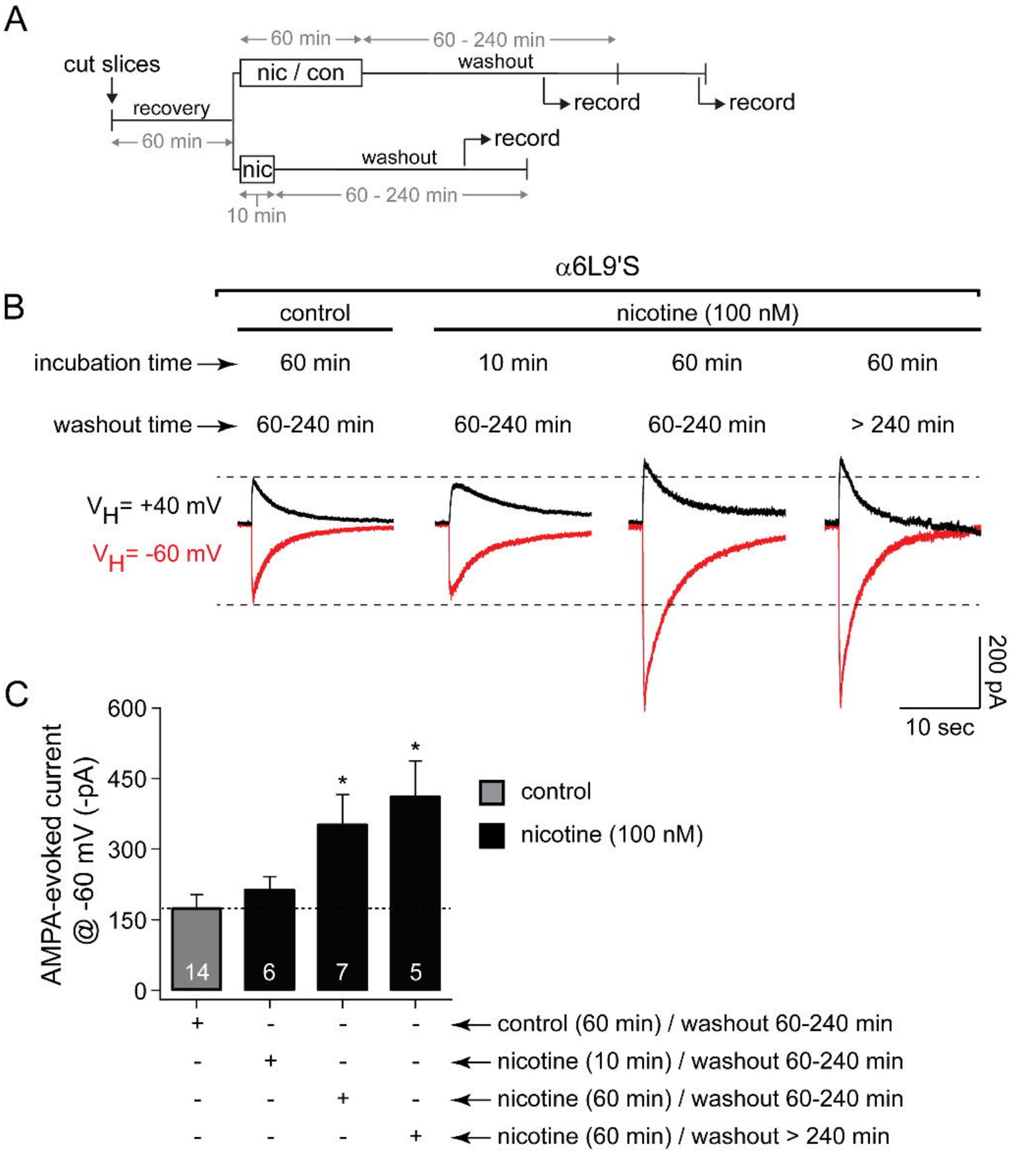
A
60 min
60 - 240 min
cut slices
nic / con
washout
record
record
recovery
60 min
record
washout
nic
60 - 240 min
10 min
α6L9'S
B
control
nicotine (100 nM)
incubation time
60 min
10 min
60 min
60 min
washout time
60-240 min
60-240 min
60-240 min
> 240 min
V_H= +40 mV
V_H= -60 mV
200 pA
10 sec
C
AMPA-evoked current @ -60 mV (-pA)
600
450
300
150
0
14
6
7
5
*
*
control
nicotine (100 nM)
+ - - - ← control (60 min) / washout 60-240 min
- + - - ← nicotine (10 min) / washout 60-240 min
- - + - ← nicotine (60 min) / washout 60-240 min
- - - + ← nicotine (60 min) / washout > 240 min

Figure 6

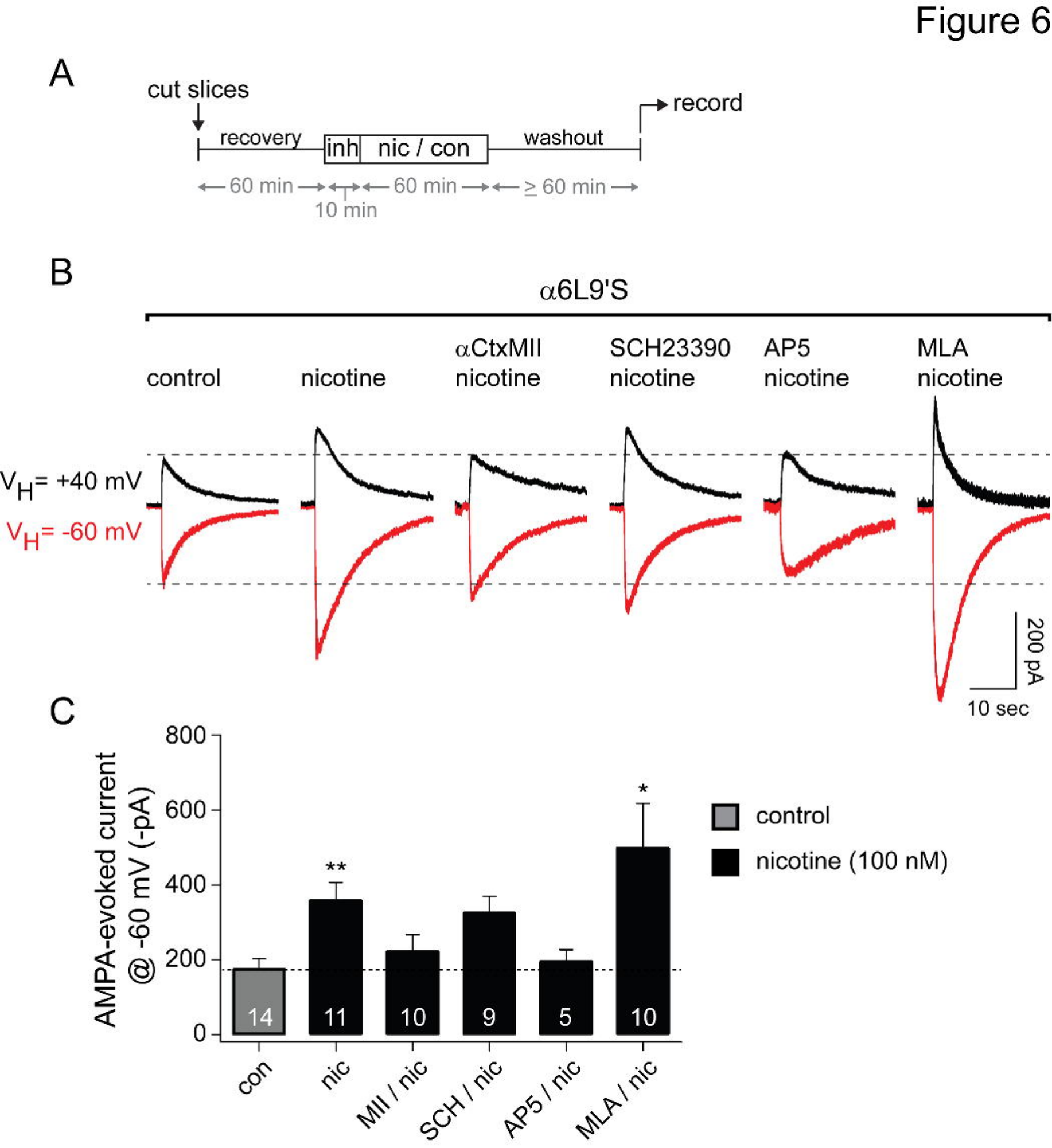
A
cut slices
record
recovery
inh
nic / con
washout
60 min
10 min
60 min
≥ 60 min
B
α6L9'S
control
nicotine
αCtxMII nicotine
SCH23390 nicotine
AP5 nicotine
MLA nicotine
V_H= +40 mV
V_H= -60 mV
200 pA
10 sec
C
AMPA-evoked current @ -60 mV (-pA)
800
600
400
200
0
**
*
14
11
10
9
5
10
control
nicotine (100 nM)
con
nic
MII / nic
SCH / nic
AP5 / nic
MLA / nic

Figure 7

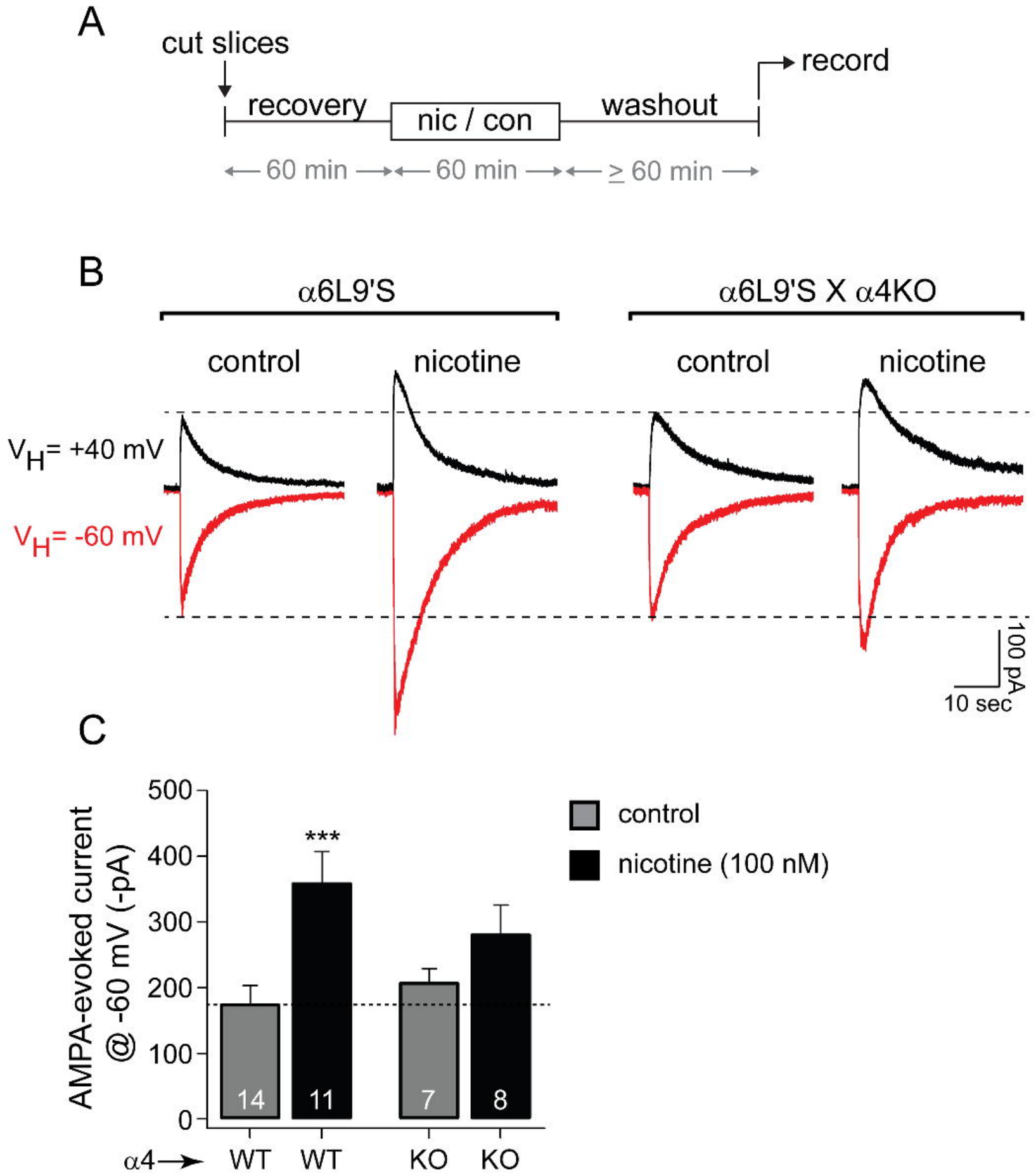
A
cut slices
record
recovery
nic / con
washout
60 min
60 min
≥ 60 min
B
α6L9'S
α6L9'S X α4KO
control
nicotine
control
nicotine
V_H= +40 mV
V_H= -60 mV
100 pA
10 sec
C
AMPA-evoked current @ -60 mV (-pA)
500
400
300
200
100
0
***
14
11
7
8
α4 →
WT
WT
KO
KO
control
nicotine (100 nM)

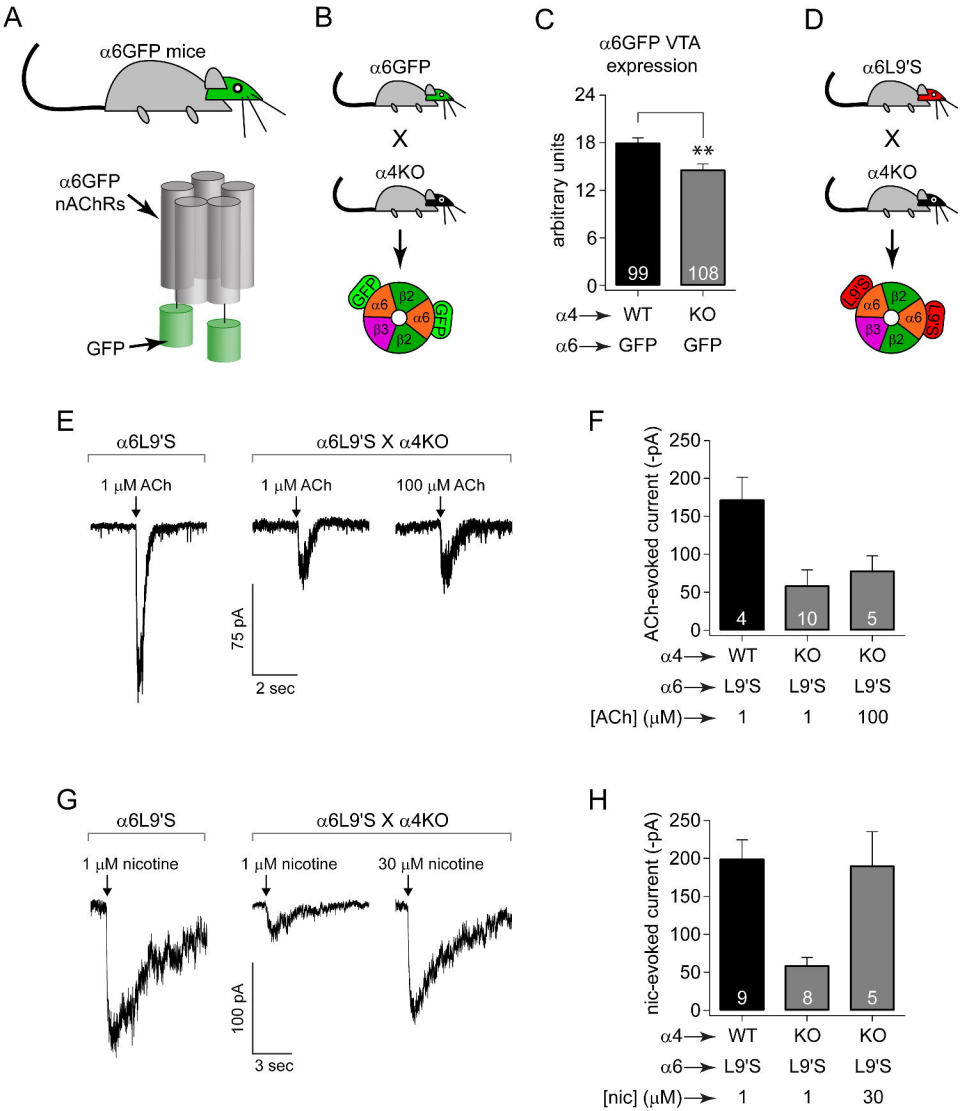
A
α6GFP mice
α6GFP
nAChRs
GFP
B
α6GFP
X
α4KO
GFP
α6
β2
α6
β3
β2
GFP
C
α6GFP VTA
expression
arbitrary units
24
18
12
6
0
**
99
108
α4→ WT KO
α6→ GFP GFP
D
α6L9'S
X
α4KO
L9'S
α6
β2
α6
β3
β2
L9'S
E
α6L9'S
α6L9'S X α4KO
1 μM ACh
1 μM ACh
100 μM ACh
75 pA
2 sec
F
ACh-evoked current (-pA)
250
200
150
100
50
0
4
10
5
α4→ WT KO KO
α6→ L9'S L9'S L9'S
[ACh] (μM)→ 1 1 100
G
α6L9'S
α6L9'S X α4KO
1 μM nicotine
1 μM nicotine
30 μM nicotine
100 pA
3 sec
H
nic-evoked current (-pA)
250
200
150
100
50
0
9
8
5
α4→ WT KO KO
α6→ L9'S L9'S L9'S
[nic] (μM)→ 1 1 30

Figure 9

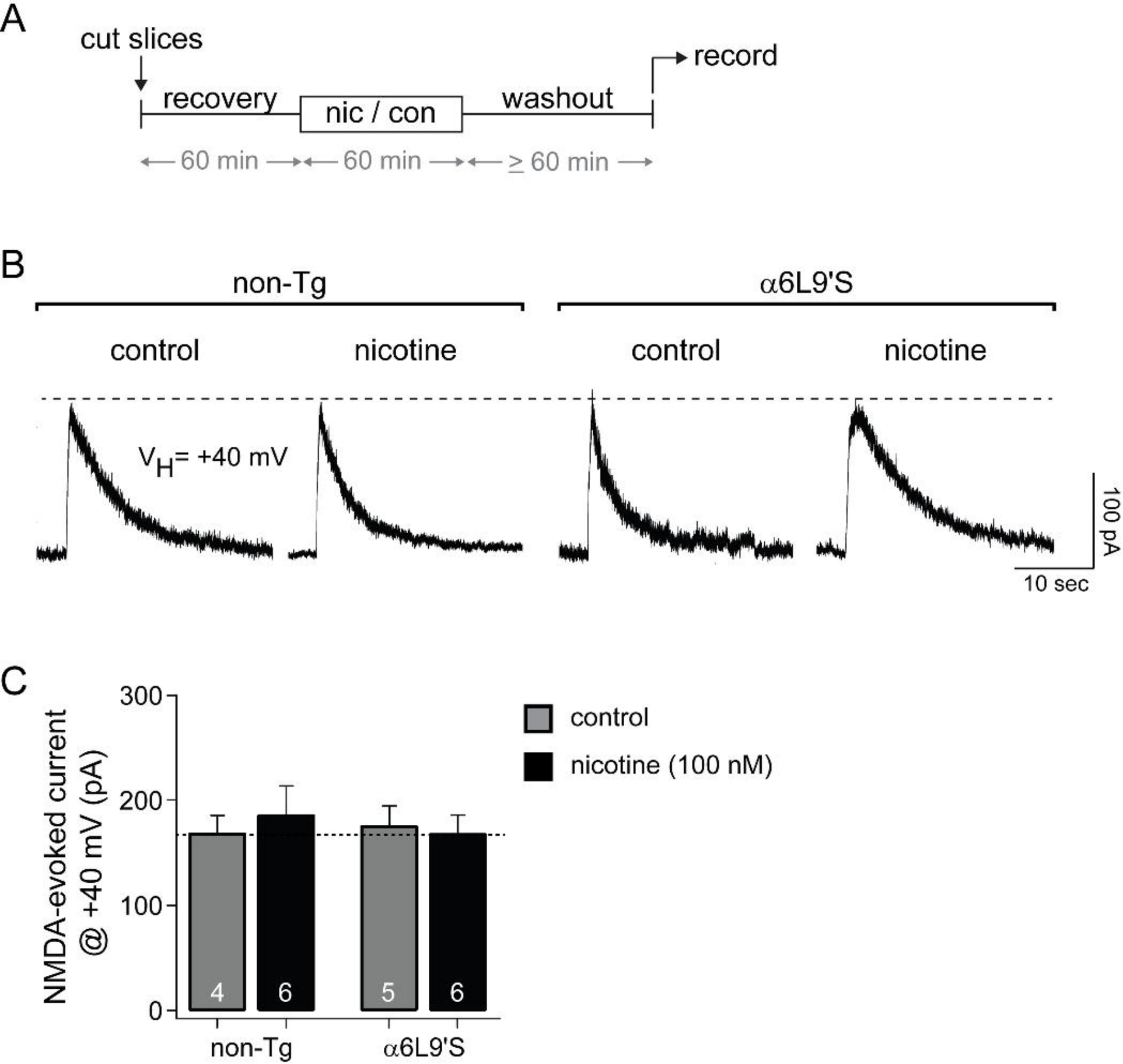
A
cut slices
record
recovery
nic / con
washout
60 min
60 min
≥ 60 min
B
non-Tg
α6L9'S
control
nicotine
control
nicotine
V_H= +40 mV
100 pA
10 sec
C
NMDA-evoked current @ +40 mV (pA)
300
200
100
0
control
nicotine (100 nM)
4
6
5
6
non-Tg
α6L9'S